Food web structure and biogeochemical processes during oceanic phytoplankton blooms: An inverse model analysis.

Robert M. Daniels[a,*], Hugh W. Ducklow[a], Tammi L. Richardson[b]

[a]*The College of William and Mary, School of Marine Science, P.O. Box 1346, Gloucester Point, VA 23062, USA. Fax: (804)684-7293*
[b]*Department of Oceanography, Texas A & M University, College Station, TX, 77843-3146, USA*
** corresponding author*

Deep-Sea Research II (submitted 06 May, 2004)

Abstract

The relationship between food web structure and function across two ocean biomes was investigated using an inverse method to recover solutions of food web carbon flows. We estimated the carbon exchanges between major assemblages within plankton food webs in the North Atlantic, using the JGOFS NABE data set (1989) and near the western Antarctic Peninsula (WAP), using the Palmer Station LTER data set, two areas exhibiting strong seasonal phytoplankton blooms. The recovery of all the potential flows of carbon allowed a system level analysis, providing insight to processes that are not measured in the field and a means of comparing food webs from different regions. In the NABE food web, the dominant carbon flows involved the microorganisms including bacterial uptake of DOC and grazing by microzooplankton and protozoans. In the WAP food web, krill grazing was the dominant flow of carbon in two contrasting years, 1996 and 1999. Salps played a significant role in altering the food web structure and function in the WAP in 1999.

A comparison between the NABE and the WAP 1996 carbon–based food webs showed key differences. Recycling and the activity of the microbial food web were much more important in the NABE food web than in the WAP. However in the WAP inverse solution, the microbial food web was just as important as the classical food web (diatoms to krill to penguins) that is traditionally believed to dominate carbon flows. Carbon flows through the NABE and WAP regions were more highly dependent on recycling than would be anticipated from the size structure of the primary producers, when analyzed using a classification scheme of Legendre and Rassoulzadegan (1986).

1. Introduction

Biological oceanographers traditionally pursue data collection on individual taxonomic or functional groups at varying levels of specificity (e. g., "phytoplankton," "diatoms," "*Nitzschia spp*," "mesozooplankton," "copepods," "*Calanus*"). It remains technically challenging to specify the biomass and key rate processes of aggregated groups, much less pertinent information for key species groups. Even less emphasis has been directed toward holistic, systems-level understanding of the composition and functioning of plankton ecosystems. Beyond a few descriptive syntheses (e. g., Landry et al., 1997; Niquil et al., 1999; Garrison et al., 2000) such efforts mostly involve numerical simulation modeling at low to moderate levels of trophic resolution (Fasham, 1995). Inverse foodweb modeling is an alternative approach, ideal for exploring the potential value hidden in observational data (Vézina and Platt, 1988). Here, we continue a systematic effort to explore the connections between food web structure and biogeochemical processes in plankton systems and in biogeochemical provinces studied by JGOFS and other programs in the past decade (Ducklow 2003; Richardson et al., *submitted*).

Ocean environments in different regions of the world have different food web structures that have adapted to the regional circulation and climate conditions (Lochte et al., 1993; McCarthy et al., 1996; Longhurst, 1998; Karl, 1999a). Thus upwelling regions are typically characterized by short or 'classical' food webs consisting of three main trophic levels: large phytoplankton, mesozooplankton grazers, and fish (Ryther, 1969), with high f-ratios and high export. Oligotrophic gyres have more complex food webs consisting of small phytoplankton, protozoans, microzooplankton, mesozooplankton grazers, and finally fish (Karl, 1999a). For example, the North Pacific Subtropical Gyre (NPSG) is considered to be a "microbial

ecosystem" dominated by prokaryotic autotrophs that are grazed upon by active protozoan and microzooplankton communities (Karl, 1999a). High latitude systems are typically characterized by short food chains dominated by diatom blooms and mismatches between production and grazing (Longhurst, 1995; Pesant et al., 1998).

Important biogeochemical processes influenced by food web structure include particle export, nutrient regeneration, and dissolved organic matter (DOM) production (Michaels and Silver, 1988). Particle export is the loss of matter from the upper ocean by sinking of organisms, attachment of detrital matter to sinking particles, and repackaging of particulate matter into the dense fecal pellets of mesozooplankton (Eppley and Peterson, 1979; Karl, 1999a). Nutrient regeneration is driven by the metabolic processes that decompose organic matter and recycle inorganic nutrients (Dugdale and Goering, 1967). Foodweb structures that promote consumption and retention of organic matter in the upper water column (e.g., small cells, complex feeding relationships) will tend to enhance nutrient regeneration (Carlson et al., 1994) and will result in lower f-ratios at the expense of export. Dissolved organic carbon (DOC) has been shown to play a significant role in export from the surface layer (Carlson et al., 1994) and also is a major resource for bacterial consumption. The lack of knowledge of DOC production and fluxes through the food web presents a significant roadblock to modeling the open ocean microbial food web (Legendre and Gosselin, 1989; Karl, 1999a). The intensity of these processes, and the chemical composition of the fluxes are influenced by the taxonomic composition and size structure of plankton foodwebs.

Previous researchers have investigated links between food web structure and these key biogeochemical processes. Eppley and Peterson (1979) related the export of particulate organic

matter out of the surface ocean to rates of primary productivity in ocean environments with very different food web structures. They calculated f-ratios for regions ranging from the oligotrophic central North Pacific to the highly productive upwelling region off the coast of Peru. The central North Pacific had a low f-ratio of about 0.05, indicating a system dominated by recycling and a relatively high residence time for nitrogen in the surface ocean. In the Peru upwelling region, the f-ratio was 0.5 with half of the total production equal to new production, fueled by nitrate upwelled from the deep waters. Legendre and Rassoulzadegan (1996) modeled links between food web structure and export, concluding that the flows of biogenic carbon are strongly influenced by the size distribution of the primary production and the matching between primary production and grazing, two key aspects of food web structure. It is not always obvious, however, that export is driven by food web structure. Rivkin et al. (1996) showed that export fluxes were similar in the Gulf of St. Lawrence even when the food webs were very (microbial vs. herbivorous).

Phytoplankton blooms often dominate ocean biogeochemistry in various ecological provinces (Watson and Whitfield, 1985; Longhurst, 1998). Here we examine the relationships between food web structure and key biogeochemical processes for two systems characterized by conspicuous spring phytoplankton blooms, the North Atlantic Ocean and the Western Antarctic Peninsula (WAP). The JGOFS North Atlantic Bloom Experiment (NABE; Ducklow and Harris, 1993) established that the bloom in this region did not necessarily correspond to the classical idea of a phytoplankton bloom dominated by large cells, having a high f-ratio and displaying mismatches between production and grazing (Garside, 1993; Harrison et al., 1993; Lochte et al., 1993; Martin et al., 1993). Mesozooplankton contributed only a small portion to the total plankton biomass and grazed a small percentage of the primary production (Dam, 1993, 1995)

and high microbial activity was observed (Ducklow et al., 1993).

In contrast to NABE, the food web in the western Antarctica Peninsula has only a few links between primary producers and large apex predators (Smith et al., 1998). The shortest path through the food web is from large diatoms to krill (*Euphausia superba*) to the apex predator, the Adélie penguin (*Pygoscelis adeliae)*. Yet some aspects of WAP foodwebs suggest more complexity. Although short paths through the food web are available, the microbial food web is present in the WAP as it is throughout the world's oceans (Fuhrman, 1989, Karl, 1999, Pomeroy, 2001). Microbial processes in the Southern Ocean are still poorly understood and not well sampled (Karl et al., 1996).

We used an inverse method (Vézina and Platt 1988) to describe plankton food web structure in these regions more fully. The inverse method uses observed data to recover estimates of all the flows within a specified food web, many of which are rarely measured. This method has been borrowed and adapted from the physical sciences (Parker, 1977; Wunsch, 1978; Wunsch and Minster, 1982), where it was used to infer ocean currents from hydrographic data. It has also been adapted to infer stocks of fish species using the program, ECOPATH (Pauly et al., 2000). It was first applied to plankton food webs by Vézina and Platt (1988) for the Celtic Sea and then later by other researchers for a variety of benthic and pelagic systems (e.g. Jackson and Eldridge, 1992; Eldridge and Jackson, 1993; Vézina and Pace, 1994; Donali et al., 1998; Niquil et al., 1998).

Our study focused in part on the role of microbial vs classical foodwebs in these two regions. We used the inverse approach to test the assumptions that the bloom in NABE was not a 'classical' phytoplankton bloom and that the microbial processes were more significant than

classical food web processes. For the western Antarctic Peninsula, we set out to better understand the relative role of the microbial food web vs. the classical food web. We compared the results from both regions to compare spring blooms of similar magnitude occurring in very different regions.

2. Methods

The inverse method uses available observed data to estimate flows in the system, which have not, or cannot, be measured. In plankton food webs, as with geophysical problems, the number of unknowns can far outnumber the independent measurements taken. More commonly, models of food webs use an *a priori* approach of assuming rate parameters and running the model over time to observe changes in the system (numerical simulation or "forward" modeling approach). Direct measurements of most of the flows and rate parameters in food webs are usually not available (Vézina and Platt, 1988). The inverse method works opposite from forward models in that it uses observations of the standing stocks and flows, along with known biological constraints to solve for unknown flows and rate parameters. The inverse method minimizes the sum of squared flows and arrives at a solution that is consistent with real data from the system, satisfies conservation of mass, and obeys the specified biological constraints (Vézina and Platt, 1988).

Carbon was the currency used in all of the models presented here. The NABE and WAP models both included the components shown in a generic ocean food web model (Figure 1), while the WAP models included additional higher trophic level components described later (Figure 2). The living components common to both models (Figure 1) included small and large

phytoplankton, bacteria, protozoans, microzooplankton, and mesozooplankton (krill in the WAP models). The nonliving components were DOC and detritus. Phytoplankton were nominally split into large (>5 μm) and small (0. 2 – 5 μm) size fractions. Legendre and Rassoulzadegan (1996) used these classes to distinguish the smaller phytoplankton that mesozooplankton can't efficiently graze from the larger phytoplankton that they do graze. Also, the large phytoplankton along with other particles >5 μm are more likely to form aggregates and sink to depth. The 'protozoans', as defined here, represented the smallest heterotrophic grazers (<10 μm) including heterotrophic nanoflagellates and ciliates (Capriulo, 1990) that feed upon bacteria and each other. 'Microzooplankton' included heterotrophic organisms between 10–200 μm such as larger nano- and microflagellates, dinoflagellates, ciliates, sarcodines and copepod nauplii (Verity et al., 1993). Heterotrophic organisms greater than 200 μm that can be captured in plankton nets, such as copepods and euphausiids, constituted the mesozooplankton (Vézina and Platt, 1988).

The mesozooplankton were restricted from grazing on the small phytoplankton and bacteria in our food webs (Figure 1). The grazers, including the protozoans, microzooplankton and mesozooplankton were allowed to consume other grazers, as long as their prey were smaller in size. All of the grazers were allowed to consume detritus. All of the living components, plus detritus, contributed to DOC. Inputs to the system were the gross primary production for large and small phytoplankton. Outputs from the system were sinking detritus, mesozooplankton production (krill, salp, penguin, and myctophid production for the WAP models) that is consumed by higher trophic levels and respiration by the living compartments.

All of the possible flows in the food web were defined by mass balance equations (Appendix A), such that the flows entering each component must equal the flows leaving, plus

any observed or assumed change in biomass of the component over the period studied (zero for steady state). Measured food web flows were used as targets for the solution, and were allowed to vary within one standard deviation of the measured or specified values (Appendix A). The boundary conditions for the model were defined using measured primary production as the input and measured sedimentation as the output for the system (Appendix A). Biological constraints (Appendix B), such as respiration and assimilation efficiency were used to keep the unknown flows within reasonable ecological and physiological boundaries (Jackson and Eldridge, 1992; Vézina and Platt, 1988). For example, the respiration of bacteria was constrained to be at least a minimum of 20% of bacterial uptake of DOC and less than or equal to a maximum limit calculated from the mass-specific power function defined by Moloney and Field (1989).

The inverse solution to the food web flows is set up as a matrix problem using linear equations describing the mass balance, boundary conditions, and measured flows of the food web. The biological constraints provide more linear equations that further constrain the solution. A Matlab program written by George Jackson (Texas A&M University; available online at http://www. ocean.tamu.edu/~ecomodel/Software/invmodel/invmodel.html) was used to find the inverse solution to the food web matrix.

Sensitivity analysis and various network analysis techniques were used to analyze model results. The input parameters to the models were varied by ± 10% in order to test the sensitivity of the model flows to small changes in the inputs. The sensitivity analysis highlights measurements that the modeled food web is sensitive to, as well as organisms and flows in the model that are sensitive to changes in input and parameter settings.

The network analysis indices used were based on the network analysis approach of

Ulanowicz (1986) and the application of network analysis to inverse models by Niquil (1998). The NETWRK program by Ulanowicz (1986), available at www.cbl.cees.edu/ /~ulan/ntwk/network.html was used to find many network analysis indices based on the model solution flows. Here we show the effective trophic levels for each living and nonliving component. Other indices used were ***F, L, and*** **Total ingestion / PP.** ***F*** is the fractional flow through a specific compartment either divided by the net primary production or the total flows through compartments with a similar trophic level. ***Fbac*** is equal to the ratio of bacterial production to net primary production (Niquil et al., 1998). ***Fpro***, ***Fmic***, ***Fmes,*** and ***Fkri*** are the ratios of the total flows through the protozoan , microzooplankton, mesozooplankton and krill compartments, respectively to the total flows through all grazer compartments (Niquil et al., 1998). The index of recycling, ***L*** is an estimate of the average number of times a carbon atom passes through the system before export (Niquil et al., 1998). Another index of recycling, the **Total ingestion / PP** is equal to the sum of all grazer ingestion flows, including bacterial consumption of DOC, divided by the net primary production.

3. Data Synthesis and Model Inputs

Model solutions are dependent on, and are required to obey, observations. Here we provide brief descriptions of the methods used in data collection and processing, necessary for understanding how the model results were constrained and derived. The original publications and Daniels (2003) should be consulted for further details.

The North Atlantic model included the basic components described above and shown in Figure 1. The western Antarctic Peninsula models include the basic components in the North

Atlantic model plus myctophids, a group of fish that have been abundant in recent years and the apex predator, the Adélie penguin (Figure 2). Krill were the only mesozooplankton grazer represented in the WAP models because they are usually the dominant zooplankton in the area (Ross et al., 1996). Salps were abundant in 1999 and were included in the 1999 inverse model, but were not observed in 1996 and so were not included for that year's model (Figure 2).

3. 1. North Atlantic Bloom Experiment (NABE)

The majority of the data for the NABE food web were taken from the May 18 –31, 1989 US JGOFS cruise on the RV Atlantis II, during the later phase of the still-active bloom. This period has the most inclusive data for the study, including in most cases daily measurements of phytoplankton production and biomass, new and regenerated production, bacterial production and biomass, microzooplankton grazing and biomass, mesozooplankton grazing and biomass, and export. Data were downloaded from http://usjgofs. whoi. edu/jg/dir/jgofs/nabe/atlantisII/ and are also available on the United States JGOFS Process Study Data 1989-1998 CD-ROM, (available from US JGOFS Office, WHOI). The measurements were integrated to 35 m, the depth of ^{234}Th-based estimates of export (Buesseler et al., 1992). Carbon measurements were averaged over the two-week observation period to arrive at mean values to be used in the inverse analysis (Table 1). The standard deviations of the daily integrated rate measurements were used to set minimum and maximum constraints on these flows. In cases where the standard deviation was not available, we chose wide ranges (e.g., 0.5 to 1.5 times the measured values) in order to avoid forcing the model into a particular result.

Regressions were performed on the biomass measurements vs. time to determine if there were significant changes over the study period. Bacterial biomass increased by 6.3 mmol C m^{-2}

d^{-1} and microzooplankton biomass increased by 9.2 mmol C m^{-2} d^{-1} (Figure 3). These changes were entered into the balance equations for bacteria and microzooplankton (Appendix A), respectively, forcing the model to account for the observed increases in these compartments.

Primary production (Figure 3) was measured *in situ* approximately every other day (Martin et al., 1993). The average primary production integrated to 35 m was 88 mmol C m^{-2} d^{-1}, nearly equal to the production integrated to the depth of the entire euphotic zone (35-50 m) of 90.4 mmol C m^{-2} d^{-1} (Martin et al., 1993). The average primary production was assumed to be split evenly between the small and large phytoplankton (Joint et al. 1993). Phytoplankton biomass (Figure 3) was estimated from Chl a (Repeta, 2003) using a C:Chl a ratio of 80 (Ducklow et al., 1993).

Bacterial production was estimated by Ducklow et al. (1993) using ^{3}H-thymidine incorporation. Bacterial biomass was estimated from daily measurements by acridine orange direct counts (Figure 3).

Dilution experiments were performed 3 times to provide grazing rates for zooplankton smaller than 200 μm, including both the protozoan and microzooplankton size classes in the models (Verity et al., 1993). Total microzooplankton biomass (Figure 3) was derived from measurements of abundance and group specific biomass of ciliates, dinoflagellates, and microflagellates (Verity et al., 1993).

Dam et al. (1993) estimated the total mesozooplankton grazing using gut fluorescence and gut clearance experiments for mesozooplankton split into three size classes: 0.2 – 0.5 mm, 0. 5 – 1. 0 mm, and 1. 0 – 2. 0 mm (Figure 3). Mesozooplankton carbon biomass (Figure 3) was measured independently from trawls (Dam, 2003).

The export from the NABE system was estimated from measurements of ^{234}Th: ^{238}U disequilibria (Buesseler et al., 1992) and represented as both low and high estimates of carbon flux at 35 m.

3. 2. *Western Antarctic Peninsula (WAP)*

The WAP measurements used for the model inputs were taken from midsummer (January) cruises in 1996 and 1999 in the Palmer LTER regional sampling grid (Figure 4a) and from inshore sites near Palmer Station, also during January. All the WAP data were obtained from the Palmer LTER website (http://pal. lternet. edu/datausepolicy_03pal. html), unless otherwise noted. January is a critical time for Adélie penguin chick development and is coincident with the crèche period, when both parents leave the chicks on land and forage, doubling the food provided to the chicks (Salihoglu et al., 2001). Data for the models were taken from stations within the foraging area of the Adélie penguins (Figure 4b). The sampling areas are defined by the seaward part of a circular area centered on Anvers Island, the home of the local Adélie colony, and with a radius equal to the foraging distance of the adult Adélies: 113 km for January, 1996 and 208 km for January, 1999 (Culik and Wilson, 1991; W. Fraser, unpublished data).

The measurements were averaged over each January to provide values to use in the models for 1996 and 1999 (Table 1). All data were integrated to a depth of 35 m, unless otherwise stated, to allow for direct comparison with the NABE results. The standard deviations of the rate measurements were used to set minimum and maximum constraints on the calculated flows. The measured biomass values were used to set the maximum constraints for respiration, so there were no minimum and maximum constraints listed for the biomasses. The measurements

for the western Antarctic Peninsula were not a time series, as in NABE, but were taken from selected stations on the regional and local sampling grids from the 1996 and 1999 cruises. Given the sampling scheme, it was not possible to estimate changes in the biomasses of food web components over the study period. It was assumed that biomass did not change over the month and the balance equations for each component were set to zero. An analysis of an inverse method applied to data sampled from a simulated plankton food web in a transient state and assuming no change in the mass balance components was shown to be just as accurate as the method applied to the same food web in steady state (Vézina and Pahlow, 2003).

Primary production for January 1996 (Figure 5) was measured to the 2% light level and data were integrated to a depth of 35 m to allow comparison with the North Atlantic models. The 2% light level was almost always above 35 m, so the integrated production was representative of the entire euphotic zone. The primary production for January 1999 was measured to the 1% light level. The primary production was integrated to 35 m, which was much shallower than the depth of the euphotic zone with an average depth for the 1% light level of 69 m. However, the average integrated primary production for the full euphotic zone (35 mmol C m^{-2} d^{-1}) was not very different from the upper 35 m (29 mmol C m^{-2} d^{-1}). The primary production in both years was split among the small (< 5 µm) and large (> 5 µm) phytoplankton, with 2/3 of the measured production assigned to the large phytoplankton and 1/3 to the small. The phytoplankton community in the Palmer region is dominated by larger cells (diatoms) during bloom conditions (Garibotti, 2003). Chlorophyll *a* in both January, 1996 and January, 1999 was measured by fluorometry and converted to carbon biomass (Figure 5) using a C:Chl ratio of 50 (Holm-Hansen and Mitchell, 1991).

Bacterial production in the WAP was estimated by the inverse routine because measured production was not available in carbon units. The bacterial production was constrained to be between the broad range of zero and fifty percent of the primary production for both 1996 and 1999, so as not to force the solution to a particular value. Bacterial biomass (Figure 5) for both January, 1996 and January, 1999 was determined from measurements of particulate lipopolysaccharide. Microzooplankton grazing was not measured as part of the Palmer LTER study. Estimates from different areas of the Southern Ocean including the Ross Sea (Caron et al., 2000), and the Atlantic sector (Becquevort, 1995; Froneman, 1996) were used to provide a wide range of potential microzooplankton grazing from 0 – 75% of primary production. Microzooplankton biomass was not measured, so the upper bound of microzooplankton respiration was left unconstrained.

Antarctic krill (*Euphasia superba*) biomass was estimated from penguin stomach content data, trawl data, and other estimates from the literature. Penguins are opportunistic visual predators that do not discriminate between different sizes of krill, so the size distribution of krill in their stomachs is a good approximation of the size distribution of krill in the area (Salihoglu et al., 2001). The average krill sizes were used to estimate the individual wet weight of an average krill, using regressions established by R. Ross and L. Quetin (unpublished data) between length and wet weight of krill measured in trawl catches. The density of krill measured in trawls was then used to find the biomass of krill. The biomass of krill was also estimated from acoustic data taken with an echo sounder within the regional grid (Lascara et al., 1999).

Krill grazing (Table 1) was estimated from a feeding relationship established in experiments during 1991 and 1992 by Ross et al. (1998). The average phytoplankton

concentration in the upper 35 m was used in the feeding relationship to estimate the mass specific feeding rate. The trawl and acoustic biomass measurements were used to find minimum and maximum population grazing estimates, respectively.

Adélie penguin grazing was estimated using counts of penguins and grazing estimates from a modeling simulation of penguin chick feeding. The total number of penguins was tallied from surveys of penguins on the islands within the vicinity of Palmer Station that were likely to feed in the Adélie foraging areas (W. Fraser unpublished data). The Adélie feeding rate, in mmol C m^{-2} d^{-1} was then found (Table 1) based on a modeling study that estimated the feeding required for Adélie chicks to acquire measured fledging weights, which are remarkably consistent from year to year (Salihoglu et al., 2001). Penguin biomass (Table 1) was estimated from penguin weights for males, females and chicks measured on Torgersen Island (W. Fraser unpublished data).

The biomass of myctophids (Table 1) was estimated using minimum and maximum densities from measurements made in 1988, as part of the AMERIEZ study in the marginal ice zone in the Atlantic sector of the Southern Ocean (Lancraft et al., 1991; Pakhomov et al., 1996). Myctophid grazing (Table 1) was then estimated using minimum and maximum mass specific grazing rates (Pakhomov et al., 1996).

Salp grazing (Table 1) was estimated from the measured abundance of salps caught in zooplankton trawl surveys in 1999. Salp grazing is only shown for 1999 because in 1996 salps were not observed in the trawls. Minimum and maximum mass specific grazing rates are from a study in the Lazarev Sea (Perissinotto and A. Pakhomov, 1998).

Export of particulate carbon was measured at a sediment trap located near Palmer Station

at a depth of 350 m (Table 1). The export at 35 m was estimated using the measurements at 350 m and assuming a normalized power function derived for open ocean environments (Martin et al., 1987): $F = F_{100} (z/100)^b$. The known export at 350 m was used to estimate F_{100} using the above equation and assuming b = - 0. 858 (Martin et al., 1987). The export at 35 m was then estimated using the above equation.

4. 0 Results.

4. 1. North Atlantic Bloom Experiment Inverse Model Results

The bacterial consumption of DOC and grazing by microzooplankton and protozoans dominated the flows of carbon in the North Atlantic inverse solution (Figure 6a and Table 2). Bacterial consumption of DOC was the largest flow (34.0 mmol C m^{-2} d^{-1}) equal to 54% of the net primary production (Figure 6a and Table 2). The microzooplankton and protozoans together dominated grazing. Microzooplankton grazing of small and large phytoplankton carbon removed 43% of the NPP (Table 2) while protozoans grazed 21% of the NPP as small phytoplankton (Table 2). Mesozooplankton grazing of large phytoplankton was equal to just 6% of the NPP. The export or e-ratio for NABE was derived by summing the sinking detritus and the mesozooplankton export (transfer of mesozooplankton to higher trophic levels not modeled or mortality) and normalizing to the primary production:

e-ratio = 0.17 + 0.03 = 0.20 (Table 2).

4. 2. Western Antarctic Peninsula 1996 and 1999 Inverse Model Results

The observed primary production in the WAP was an order of magnitude greater in 1996

than in 1999 and the relative magnitudes of flows recovered in the modeled food webs reflected this disparity. The largest flows within the food web, inferred by the 1996 carbon model inverse solution, were krill grazing and respiration, equivalent to 42 and 20% of the NPP, respectively (Figure 7a and Table 3). The next most important flows were microzooplankton respiration (16% of NPP) and bacterial ingestion of DOC (15% of NPP), which channeled a significant amount of carbon into the microbial food web. Thus while short food web processes were the dominant flows, microbial food web processes were important as well.

The estimated flows for the upper trophic levels in the 1996 carbon model including penguins and myctophids were much smaller than for the lower trophic levels. Myctophids consumed 1.08 mmol C m^{-2} d^{-1} of krill equal to 1% of the net primary production and the penguins consumed 0.11 mmol C m^{-2} d^{-1} of krill or 0.1% of the production, an order of magnitude less than myctophids (Table 3).

The particulate carbon export from the top 35 m was equal to 18 mmol C m^{-2} d^{-1} or 21% of the primary production (Table 3). The export of krill, representing krill production that can be consumed by higher trophic levels or else sink when the krill die, was an additional 17% of the primary production. The estimated export (e-) ratio was equal to the sum of the particulate export, the krill export, the penguin export and the myctophid export all normalized to primary production:

e-ratio = 0.20 + 0.17 + 0 + 0.004 = 0.37.

Krill and microzooplankton grazing were the largest flows within the food web in the carbon model inverse solution for 1999 (Figure 7b and Table 3). Salps also played a significant role in the food web. Their total consumption of all diet components was about equal to krill

grazing of phytoplankton (each 21% of NPP; Table 3). Other large flows in the food web included large phytoplankton to detritus, microzooplankton respiration, and bacterial respiration equal to 16, 15, and 15% of the primary production, respectively. A significant amount of carbon was processed by the microbial food web in 1999 as well as in 1996.

The particulate carbon export sinking out of the top 35 m was 18% of the primary production, similar to the 1996 export normalized to the NPP (21%), but an order of magnitude lower in absolute terms. The 1999 overall e-ratio of 0. 35 were very similar to the 1996 e-ratio of 0. 37. With the significant exception of the presence of salps in 1999, the overall structure of the foodwebs was similar, with equivalent fractions of the NPP allocated between the short and microbial foodwebs and to export in both years.

4. 3. North Atlantic vs. Western Antarctic Peninsula

A direct comparison was made between the WAP 1996 and NABE carbon models in order to investigate differences in the trophic functioning expressed in the two regions, as a result of the different food web structures. A direct comparison between the WAP 1996 carbon inverse solution and the NABE carbon inverse solution is meaningful because the inferred primary production in the models was similar: 63 mmol C m^{-2} d^{-1} for NABE and 89 mmol C m^{-2} d^{-1} for the 1996 WAP carbon model. Also, many of the results of the WAP 1996 and 1999 models were similar with respect to the food web flows normalized to the primary production. A new condensed model for the WAP, with the same components as the NABE model, except for krill replacing the mesozooplankton in the WAP, was made for the comparison (Figure 6b). The higher trophic levels including myctophids and penguins were not included in the condensed model. The same input measurements and assumptions used for the original WAP 1996 carbon

model shown in Table 1 were used in the condensed model, except for the higher trophic level measurements that were not required.

The 1996 WAP condensed model inverse solution flows were almost identical to the flows in the original 1996 carbon model (Tables 3 and 4). Only two flows changed by more than 1%. The krill consumption of protozoans was 35% smaller in the condensed model, but was less than 1% of the primary production in both models. The krill export flow was 7% larger in the condensed model than the full model, but increased just 1% with respect to the primary production.

The largest flow within the 1996 WAP condensed food web was the krill grazing of large phytoplankton, while the largest flow within the NABE food web was bacterial ingestion of DOC (Table 2 and Figure 6). The sum of microzooplankton and protozoan grazing in the NABE model was twice as great as in the WAP model relative to primary production (Table 2). NPP-normalized krill grazing in the WAP model was 7 times larger than mesozooplankton grazing in the NABE model.

DOC release by phytoplankton was equal to 6% of the primary production in the WAP model but a much larger portion was required to sustain the bacteria in the NABE model (22% of NPP; Table 2), even though the bacterial flow was less constrained in the WAP model. The bacteria were much more active in the NABE model, ingesting about 4 times as large a share of the NPP as in the WAP (Table 2).

The sinking particulate carbon export leaving the surface ocean was similar for the two models, 20% for the WAP and 17% for NABE. Krill export production, representing predation of krill by higher trophic levels like Adélies or an increase in the krill biomass, was 18% of the

primary production, much higher than the 3% export production from mesozooplankton in the NABE model. The estimated e- ratios for the two systems are NABE: e-ratio = 0.17 + 0.03 = 0.20 and WAP: e-ratio = 0.20 +0.18 = 0.38.

4. 4. Comparison of short food web vs. microbial food web

The short diatom-krill-predator food chain is believed to be the most significant pathway for carbon in coastal waters of the Southern Ocean (Huntley et al., 1991). In contrast the microbial food web is now believed to play an active role in the North Atlantic bloom (Ducklow et al., 1993; Harrison et al., 1993; Lochte et al., 1993). The relative activities of the short or classical food chain and microbial food webs are given for the WAP 1996 and NABE carbon models in Table 4. All of the flows within the short food web that lead to export out of the surface ocean through sinking or transfer to higher trophic levels were summed. The flows within the microbial food web were also summed, including all flows between the microbial organisms and their interactions with the detritus and DOC pools. The ratio of microbial to short food web flows was 1.0 for the WAP solution, suggesting equal activity by each assemblage. In NABE, the microbial food web was 11 times more active than the short food web. The krill were the main contributor to the short food web flows in the WAP model. Myctophids and Adélie penguins, not included in this condensed model, consumed an amount of krill equal to 1.1% of the primary production in the original model.

In the NABE model, large phytoplankton, microzooplankton and bacteria made the largest contributions to the DOC pool and bacteria were one of the biggest contributors to their own diet (Figure 8). In the WAP model, krill and large phytoplankton were the biggest contributors to the DOC pool and sizable inputs were received from all the living components

except for bacteria (Figure 8). Particle decay from detritus contributed 13% of the DOC pool in the NABE solution, but did not contribute to the DOC pool in the WAP solution. Even though microbial components were much less constrained in the WAP solutions, they appear to make up a relatively minor part of the system, compared to the NABE solution.

4. 5. Comparison of network analysis indices

Network analysis indices were used to further explore the relative activity of each living and nonliving compartment. A comparison of these trophic indices for the 2 models indicates that bacterial production was much greater in NABE, where it accounted for 23% (***Fbac*** = 23%) of the primary production vs. 1% (***Fbac*** = 1%) in the WAP model (Table 5). The dominance of krill in the WAP was evident with the krill processing 52% ($\boldsymbol{F}_{kri}$ = 52%) of the total carbon passing through all the grazers (Table 5). The dominance of microzooplankton and protozoans in the North Atlantic was obvious with the total throughput of microzooplankton and protozoans equal to 88% (***Fmic*** = 48%, $\boldsymbol{F}_{\boldsymbol{pro}}$ = 40%) of the total carbon passing through all the grazers (Table 5). For the North Atlantic model, 54% of the primary production passed through the DOC pool while in the WAP model, just 14% of the primary production cycled as DOC. In both models, 25% of the primary production passed through the detritus pool.

The recycling index, **L** and the **Total Ingestion / PP** indicated greater recycling in the North Atlantic than the western Antarctic Peninsula. The average carbon atom cycles within the North Atlantic food web 2.2 times before exiting through respiration or sinking, while **L** for the western Antarctic Peninsula is 1.4 (Table 5). The **Total Ingestion / PP** indicates that in the North Atlantic food web, zooplankton and bacteria process 140% of the primary production, indicating a strong reliance on recycled carbon (Table 5). In the western Antarctic Peninsula

food web, the zooplankton and bacteria process 100% of the primary production, indicating somewhat less reliance on recycled carbon (Table 5).

The effective trophic levels found using the NETWRK program (Ulanowicz, 1986) showed a simpler food web for the WAP than for NABE (Table 6). The large and small phytoplankton, detritus, and DOC compartments are all arbitrarily assigned trophic levels of 1. In the WAP, the protozoans, microzooplankton, and krill all fed at trophic levels close to 2 (Table 6). In the NABE solution, a more complex picture was evident, with the grazers feeding at trophic levels farther from 2. The mesozooplankton had a trophic level as high as 2.49, gaining half of their diet from protozoans and microzooplankton.

Overall, these analyses of the flow network solutions suggest a microbe-dominated bloom in the North Atlantic with high reliance on recycling and active detrital pools (particulate and dissolved), while the opposite tended to be the case for the WAP. The Antarctic system was dominated by larger organisms, little activity in the microbes and detritus pools, and little dependence on recycling. The activity of the particulate detritus pool was 25% of NPP in both models and in the WAP there was consumption of detritus by zooplankton but not in NABE.

4. 6. Sensitivity Analysis

The input parameters to the NABE carbon model were successively varied by ±10% and the inverse solution was recalculated for each change to assess the sensitivity of the model to these variations. The input parameters that had the greatest effect on the carbon solution were the large and small net primary production (Figure 9a), and microzooplankton grazing (Figure 9b). The ±10% changes in these parameters caused greater than 10% changes in 12 to 17 of the 36 foodweb flows (Figures 9a, 9b) The ±10% changes in the bacterial production each caused the

same 8 flows to change by more than 10% (Figure 9b). The flows that were the most sensitive to changes in the input parameters were small phytoplankton to detritus and the mesozooplankton consumption of microzooplankton. Small phytoplankton to detritus increased 450% with an increase in 10% on the net small primary production and decreased to 0 with a decrease of 10% in the net small primary production (Figure 9a). Mesozooplankton consumption of microzooplankton increased 95% with a decrease of 10% in the net large primary production and decreased by about 40% with increases in both the net small and large primary production (Figure 9a). Changes in the input parameters also brought about the consumption of detritus in some cases. In the original solution the consumption of detritus by all three zooplankton size classes was zero. Increases in small and large primary production resulted in positive, though low rates of detritus consumption. The increase in production supplied a larger particulate detritus pool that was capitalized on by the grazers. Also, a decrease in the microzooplankton grazing rate resulted in positive, low rates of detritus consumption. When the availability of live prey was reduced, the modeled grazers necessarily turned to detritus to satisfy their energy demands.

The WAP 1996 condensed model was sensitive to the same input parameters as in the complete model for 1996 and sensitivity was similar for 1999. Changes in the large and small net primary production also had the greatest effects on the flows, as in the NABE model, with ±10% changes in 23-25 of the 36 foodweb flows, respectively (Figure 10a). The WAP model was more sensitive to changes in large and small net primary production than the NABE model. Changes in the bacterial production also had significant effects on the flows, as seen in the NABE model. The increase of 10% in the minimum bacterial production brought about changes of greater than 10% in 13 of the flows (Figure 10b). The changes in the krill minimum grazing brought about

changes greater than 10% in 6 of the flows, with the 10 % increase in grazing and 4 of the flows with the decrease. The flows that were most sensitive to input changes were flows that were not measured, but estimated by the inverse method. The most sensitive flows included the krill consumption of protozoans and the large phytoplankton release of DOC (Figure 10). The krill consumption of detritus was zero in the original solution, but the increase in net large phytoplankton production increased the krill's consumption to 3.3 mmol C m^{-2} d^{-1} (8 % of their total ingestion) and the decrease in krill minimum grazing increased the consumption to 1.18 mmol C m^{-2} d^{-1}.

5. Discussion

5.1. Accuracy of the model results.

Inverse model results represent extrapolations of food web structure from a small set of measured flows and a larger set of constraints and mass balance considerations. There is a large (potentially infinite) number of solutions consistent with the observations and constraints, and the question arises as to the accuracy and realism of the model solutions. Some criterion is needed to select the best solution. The standard criterion in almost all geophysical and ecological inversions is the solution that minimizes the sum of the squares of the estimated components (the food web exchanges or flows in ecological applications). As discussed at length in Vézina and Pahlow (2003), for ecosystem inversions this amounts to evening out the flows in a system, tending to increase small flows and decrease larger ones. It is not possible to assess empirically the accuracy of an inverse solution without a reliable and comprehensive set of measurements of flows for some system. Vézina and Pahlow (2003) addressed this problem by subsampling flow

data from a numerical simulation model of a generic plankton system, and using these subsets as "observations" to obtain inverse solutions, then comparing the estimated flows to the original simulation results. They found that the inverse method provided substantially accurate representations of the original data under a wide variety of conditions.

Vézina and Pahlow (2003) tested their inverse methodology by sampling from steady-state simulations representing winter, spring and summer conditions, and from three stages of a transient simulation similar to a phytoplankton bloom. Although reasonably accurate representations of the original systems were obtained under all conditions, the inverse results proved to be less accurate as systems evolved from winter toward summer. Winter-spring conditions, characterized by less recycling and higher export were more accurately reproduced than summer conditions with greater recycling, less export (lower e-ratios) and more complex foodwebs. Transient states produced more accurate results than the steady-state cases. In most solutions, the inverse solutions tended to overestimate flows of smaller magnitude and underestimate larger flows. Their findings have several implications for our study.

First, phytoplankton blooms are emblematic of non-steady state plankton systems. Inverse solutions have tended to assume steady state due to the frequent use of snapshots of data. Vézina and Pahlow's (2003) results imply that inverse solutions for phytoplankton blooms are not *a priori* likely to be in great error, just because they are not near the steady state. The opposite seems to be the case. Second, their finding that inverse approaches worked better on winter-spring systems with lower recycling implies that the NABE and WAP systems are good cases for application of this methodology. It is true that the NABE data implied a bloom system with larger than expected recycling; and to the extent this was so, the inverse solution may be

less accurate than the WAP case, with low recycling. Finally, Vézina and Pahlow (2003) suggested that inverse solutions tended to even out flows in the recovered solutions. Our solutions for both NABE and WAP exhibited flows with a wide range of magnitudes. That is, both systems were characterized by very large and very small flows (e.g., krill grazing and bacterial production in the WAP; and bacterial production and mesozooplankton grazing in NABE). If the inverse method behaved in our solutions as it did for Vézina and Pahlow (2003), our modeled flows appear to be robust representations of the real systems.

5. 2. Comparison of NABE and WAP Food Webs

Krill were the dominant organisms affecting the flow of carbon in the WAP food web and microbial organisms were dominant in the North Atlantic. The greatest flows within the WAP model were related to krill, while the greatest flows within the NABE model were bacterial ingestion and microzooplankton grazing. The dominance of krill is not surprising given that they usually dominate the zooplankton biomass in the WAP (Ross et al. 1998). In 1996 krill biomass was 227 mmol C m^{-2} (Table 1) vs. the mesozooplankton biomass of 7 mmol C m^{-2} (Table 1) in the North Atlantic in May 1989. The krill biomass was equal to almost 1/3 of the phytoplankton biomass in the WAP.

Active recycling was evident in the North Atlantic model, while only weak recycling was seen in the western Antarctic Peninsula model. In the NABE model, the microbial food web flows processed about 11 times more carbon than the short food web. In the WAP model, the short food web and microbial food web flows processed equal amounts of carbon, even though the short food web has traditionally been thought to be dominant in the Southern Ocean and other marginal ice zone systems (Huntley et al. 1991).

Bacterial production was much greater in the NABE food web. In the WAP model, bacterial production was just 1% of the NPP and balanced by predation (bacterivory), solely carried out by the protozoans (Table 2). In the NABE model, bacterial production was equal to 26% of the NPP and was equal to the increase in the bacterial biomass (Table 1), plus the consumption of bacteria by protozoans and microzooplankton and the loss to detritus (Table 2). The bacterial consumption of DOC was about 4 times greater in the NABE model, 54% of primary production vs. 14% for the WAP. These results for the WAP agree in part with earlier observations of low bacterial production during the spring bloom in the Gerlache strait, just north of the Palmer area (Karl et al. 1999b). High grazing rates on bacteria were measured in dilution experiments in areas of high phytoplankton biomass during the bloom (Karl et al. 1999b). The WAP model showed very low grazing of bacteria, equal to just 1% of the primary production but equal to 100% of the bacterial production. Despite low bacterial production, the bacteria still played a relatively active role in the food web by ingesting 14% of the primary production as DOC and respiring most of this uptake (13%). Large ranges were assigned to the constraints for bacterial production and microzooplankton grazing in the WAP, because these processes are highly variable across the world's oceans and not well understood in the Southern Ocean (Caron et al., 2000; Froneman and Perissinotto, 1996; Becquevort, 1995; Karl, 1996). The microzooplankton grazing inferred by the inverse method was 21% of the primary production in 1996 and 26% in 1999. The power of the inverse method is evident when it provides an estimate of microzooplankton grazing that would not have been known otherwise and was constrained between such a large range of 0 and 75% of the primary production.

The estimated e-ratio of 0.38 for the WAP model was about twice as high as in the NABE model (e = 0.20), with krill export production equaling 18% the WAP primary

production. In the WAP 1996 full carbon model, penguins and myctophids together consumed just 1% of the primary production in the form of krill. This left 17% of the primary production that could go to an increase in krill biomass or could be passed up the food web to other (unmodeled) predators. Baleen whales consume an estimated 10% of krill production in the Southern Ocean (Laws, 1985) and could consume some of this krill production. The krill production could have also been uneaten and increased the krill biomass. The model assumed no change in the krill biomass over the month of the study. The month of January is during the summer bloom and krill biomass is highly variable across seasons with up to an order of magnitude increase from fall/winter to spring /summer (Lascara et al., 1999), so a significant increase in krill biomass is possible.

The modeled e-ratio of 0.20 for NABE was lower than the value of 0.45 estimated by Martin (1993) from floating sediment traps. The model is more consistent with the conclusions of Garside and Garside (1993), who suggested that not all the new production was exported, but remained in the food web during the observation period. Our solution accounted for a sink for this unrealized export with the inclusion of the observed increases in biomass of bacteria and microzooplankton. The bacterial biomass increase of 6 mmol C m^{-2} d^{-1} and the microzooplankton increase of 9 mmol C m^{-2} d^{-1} were included in the model (Table 1). When added to the NABE model e-ratio, they give an estimate of 0.20 (e-ratio) + 0.14 (microzooplankton increase) + 0.10 (bacterial increase) = 0.44, almost identical to the Martin sediment trap e-ratio of 0.45. Nonetheless the model apportioned the new production differently than was implied by the floating sediment trap data. We used ^{234}Thorium to constrain the particle export in NABE, which tended to provide lower estimates than the traps (Buesseler et al., 1992).

Other food web flows that were inferred by the inverse method that are not otherwise known include interactions with the detrital pools. In both the NABE and WAP 1996 models, the total throughput in the detritus pool was about 1/4 of the primary production. In an inverse analysis of a plankton food web off Southern California, Jackson and Eldridge (1992) also found detritus was an active component, receiving large contributions from sinking phytoplankton and making significant contributions to the dissolved organic matter pool. In the NABE carbon solution, the dissolution of detritus made up 13% of the input to the DOC pool. In an inverse analysis of a plankton food web of the Takapoto Atoll in French Polynesia, Niquil et al. (1998) suggested that detritus played an important role providing food for all of the zooplankton components. In the NABE carbon solution there was no consumption of detritus by zooplankton, however in an independent nitrogen solution (Daniels 2003) all of the zooplankton components consumed detritus. This discrepancy (carbon-free detritus) is not possible in nature and future solutions should use a C:N ratio to force the carbon and nitrogen solutions to be more consistent with each other. In the WAP models, detritus was consumed by almost all of the zooplankton components in 1996 and all except for microzooplankton in 1999.

5. 3. Classification of Food Webs

Once the complete pattern of flows in a system is determined, different systems can be classified according to various schemes. Legendre and Rassoulzadegan (1996) described three pathways for carbon flow through a food web; the sinking of ungrazed phytoplankton, food web transfer, and recycling. They related these three food web processes to the size structure of the phytoplankton and matching of phytoplankton production with grazing. Legendre and Rassoulzadegan derived analytical solutions for the proportion of the primary production

allocated to each of the three pathways based on the ratio of large phytoplankton production to total phytoplankton production, $\mathbf{P_L/P_T}$, and the matching between phytoplankton production and grazing, **M**. They used values from the literature to estimate the magnitude of these food web functions for 5 different types of food webs. The food web types ranged along a continuum of decreasing ratios of export to primary production. At one extreme is the sinking of ungrazed cells, representing a food web with high primary production that is not matched by grazing. At the other extreme is the microbial loop, an almost closed system with near zero input of primary production, consisting of bacteria and protozoans. In between the two extremes in order of decreasing export/ production are the herbivorous, multivorous, and microbial food webs. The herbivorous food web is dominated by large phytoplankton production and grazing by mesozooplankton, while small phytoplankton cells and microbial grazers dominate the microbial food web. The multivorous food web includes equal roles of large and small phytoplankton and herbivorous and microbial grazing.

Using measurements of the size structure of the phytoplankton, $\mathbf{P_L/P_T}$ and estimates for the degree of matching, **M,** Legendre and Rassoulzadegan solved for the 3 pathways of carbon flow in the 5 different food web systems and compared the results to estimates from the literature. They found good agreement between their derived values of food web function and the estimates from the literature (coefficient of determination, $R^2 = 0.83$), supporting their assumption that the size structure of the phytoplankton and degree of matching strongly determined food web structure.

The 3 food web functions listed in Table 2 in Legendre and Rassoulzadegan (1996) for five different types of food webs provide a baseline to compare estimates of these functions from

the WAP carbon models and the NABE carbon model (Table 7). The food web transfer described by Legendre and Rassoulzadegan (1996), $\mathbf{F_T/P_T}$, includes any carbon passed up the food chain that is exported out of the surface ocean by sinking or transfer to higher trophic levels. This includes the fecal pellets and export production of mesozooplankton or krill. In the WAP models it also includes myctophid and salp (for 1999) fecal pellets and export production. Penguin export production is also included, but not penguin feces, which are mostly left on land. The recycling pathway, $\mathbf{R_T/P_T}$ was found by subtracting the total export equal to the sum of $\mathbf{F_T/P_T}$ and $\mathbf{D_T/P_T}$, indicating the fraction of ungrazed, sinking phytoplankton, from the total net primary production, equal to 1.0.

The NABE carbon model has food web functions lying somewhere between the microbial food web and the microbial even though the segregation of the primary production $\mathbf{P_L/P_T}$ of 0.5 is much higher than assumed for these systems. The recycling pathway consumes a high proportion of the primary production, $\mathbf{R_T/P_T}$ = 0. 9, putting the North Atlantic food web between the microbial food web and the microbial loop. The food web transfer, $\mathbf{F_T/P_T}$ of 0.03 is very low, putting the food web close to the microbial loop, while the sinking phytoplankton pathway, $\mathbf{D_T/P_T}$ of 0.07 is slightly closer to the multivorous food web value (0.1) but not far from the microbial loop and food web values (each equal to 0).

The WAP 1999 and 1996 models show similar results to the Legendre and Rassoulzadegan (1996) analysis. The WAP 1996 carbon model is closest to the multivorous food web, but still (surprisingly) leaning towards the microbial food web. The recycling pathway, $\mathbf{R_T/P_T}$ of 0.63 is slightly higher than for the multivorous food web. The food web transfer pathway, $\mathbf{F_T/P_T}$ of 0.2 is equal to that of the microbial food web and the sinking pathway $\mathbf{D_T/P_T}$

is slightly higher than the multivorous food web value. The WAP 1999 model is also close to the multivorous food web though leaning towards the microbial food web. The recycling pathway, $\mathbf{R_T/P_T}$ = 0.68 is about halfway between the recycling in Legendre and Rassoulzadegan's multivorous food web and microbial food web. The food web transfer, $\mathbf{F_T/P_T}$ is close to the microbial food web value, while the sinking phytoplankton pathway, $\mathbf{D_T/P_T}$ is equal to the multivorous food web value.

The inverse solutions give values of the food web functions that are somewhat different than would be expected using Legendre and Rassoulzadegan's (1996) assumptions of size distribution of primary production. The size distribution of primary production for each of the inverse models indicate food webs lying somewhere between the multivorous and herbivorous food web. However, the food web functions calculated from the inverse model results put the North Atlantic food web somewhere between the microbial food web and microbial loop and the western Antarctic Peninsula food web close to a multivorous food web leaning towards the microbial loop. The matching parameter used by Legendre and Rassoulzadegan is an arbitrary parameter that is not related directly to measurements. For NABE, the matching between grazers and phytoplankton was likely high because the fast growing microzooplankton and protozoans dominated the grazing and there was no increase in phytoplankton during the study. This high degree of matching would push the NABE food web towards higher recycling in the direction of the microbial loop. For the WAP, the dominance of krill grazing would give a lower degree of matching than in NABE because of the relatively slower growth of krill to microzooplankton and push the food web towards the extreme of sinking of ungrazed cells. These findings reveal a bias in both of the inverse solutions towards the microbial loop extreme. The assumptions from Legendre and Rassoulzadegan are based on only a few food webs, so it is possible that with data

from more systems these descriptions of food web types would be different and biased towards higher recycling. It is also possible that model solutions like ours, where all flows are known, give different results than observed systems for which our knowledge remains incomplete.

Acknowledgements.

We are grateful to George Jackson for providing his software and much guidance during this project. Bill Fraser, Robin Ross and Langdon Quetin provided data and answered questions about the WAP system. This research was supported by US JGOFS Synthesis and Modeling Project NSF grants, OCE-0097237 to HWD and OCE-0097296 to G. Jackson (TAMU). Also the work was supported by NSF grant ONR 00014210370 (NOPP) subcontract to HWD. This is US JGOFS Contribution YYYY.

Appendix A. Mass balance equations, boundary conditions, and observation equations.

Flows are indicated as a 'C' for carbon followed by the compartment of origin (with a 3 letter designation), followed by 'TO', then followed by the destination compartment. Large phytoplankton gross production and small phytoplankton gross production are gpL and gpS, respectively.

Mass Balance Equations for NABE carbon model compartments.

Large Phytoplankton (phL): CgpLTOphL – CphLTOres – CphLTOmic – CphLTOmes – CphLTOdet – CphLTOdoc = 0 mmol $Cm^{-2}d^{-1}$

Small Phytoplankton (phS): CgpSTOphS – CphSTOres – CphSTOpro – CphSTOmic – CphSTOdet – CphSTOdoc = 0 mmol $Cm^{-2}d^{-1}$

Bacteria (bac): CdocTObac – CbacTOres – CbacTOpro – CbacTOmic – CbacTOdet = 6.3 mmol $Cm^{-2}d^{-1}$

Protozoans (pro): CbacTOpro + CphSTOpro + CdetTOpro – CproTOmic – CproTOmes – CproTOres – CproTOdet – CproTOdoc = 0 mmol $Cm^{-2}d^{-1}$

Microzooplankton (mic): CphLTOmic + CphSTOmic + CproTOmic + CbacTOmic + CdetTOmic – CmicTOres – CmicTOmes – CmicTOdet – CmicTOdoc = 9.2 mmol $Cm^{-2}d^{-1}$

Mesozooplankton (mes): CphLTOmes + CproTOmes + CmicTOmes + CdetTOmes – CmesTOres – CmesTOdet – CmesTOdoc – CmesTOext = 0 mmol $Cm^{-2}d^{-1}$

Detritus (det): CphLTOdet + CphSTOdet + CphSTOdet + CproTOdet + CmicTOdet + CmesTOdet + CbacTOdet – CdetTOpro – CdetTOmic – CdetTOmes – CdetTOdoc - CdetTOext = 0 mmol $Cm^{-2}d^{-1}$

DOC (doc): CphLTOdoc + CphSTOdoc + CproTOdoc + CmicTOdoc + CmesTOdoc + CbacTOdoc + CdetTOdoc – CdocTObac = 0 mmol $Cm^{-2}d^{-1}$

Boundary conditions for NABE carbon model.

Minimum Large Phytoplankton Primary Production: CgpLTOphL – CphLTOres ≥ 31.5 mmol $Cm^{-2}d^{-1}$

Mazimum Large Phytoplankton Primary Production: CgpLTOphL - CphLTOres = 56.5 mmol $Cm^{-2}d^{-1}$

Minimum Small Phytoplankton Primary Production: CgpSTOphS – CphSTOres ≥ 31.5 mmol $Cm^{-2}d^{-1}$

Maximum Small Phytoplankton Primary Production: CgpSTOphS - CphSTOres = 56.5 mmol $Cm^{-2}d^{-1}$

Minimum Export: CdetTOext ≥ 7.7 mmol $Cm^{-2}d^{-1}$

Maximum Export : CdetTOext = 23.6 mmol $Cm^{-2}d^{-1}$

Observation equations for NABE carbon model.

Minimum Microzooplankton Grazing: CphLTOmic + CphSTOpro + CphSTOmic ≥ 40.5 mmol $Cm^{-2}d^{-1}$

Maximum Microzooplankton Grazing: CphLTOmic + CphSTOpro + CphSTOmic = 121.5 mmol $Cm^{-2}d^{-1}$

Minimum Mesozooplankton Grazing: CphLTOmes ≥ 1.2 mmol $Cm^{-2}d^{-1}$

Maximum Mesozooplantkon Grazing: CphLTOmes = 3.6 mmol $Cm^{-2}d^{-1}$

Minimum Bacterial Production: CbacTOpro + CbacTOmic + CbacTOdet = 17.0 mmol $Cm^{-2}d^{-1}$

Maximum Bacterial Production: CbacTOpro + CbacTOmic + CbacTOdet ≥ 23.0 mmol $Cm^{-2}d^{-1}$

Mass Balance Equations for WAP 96 (condensed and full) and WAP 99 carbon inverse models. The compartments and flows with italic text are in the WAP 96 and 99 full models. The compartments and flows with bold text are in the WAP 99 model only.

Large Phytoplankton (phL): CgpLTOphL – CphLTOres – CphLTOmic – CphLTOkri – CphLTOdet – CphLTOdoc – **CphLTOsal =** 0 mmol $Cm^{-2}d^{-1}$

Small Phytoplankton (phS): CgpSTOphS – CphSTOres – CphSTOpro – CphSTOmic – CphSTOdet – CphSTOdoc – **CphSTOsal =** 0 mmol $Cm^{-2}d^{-1}$

Bacteria (bac): CdocTObac - CbacTOres – CbacTOpro – CbacTOmic – CbacTOdet – CbacTOdoc – **CbacTOsal =** 0 mmol $Cm^{-2}d^{-1}$

Protozoans (pro): CbacTOpro + CdetTOpro + CphSTOpro - CproTOmic – CproTOkri – CproTOres – CproTOdet – CproTOdoc – **CproTOsal =** 0 mmol $Cm^{-2}d^{-1}$

Microzooplantkon (mic): CphLTOmic + CphSTOmic + CproTOmic + CbacTOmic + CdetTOmic + CbacTOmic + CdetTOmic – CmicTOres – CmicTOkri – CmicTOdet – CmicTOdoc – **CmicTOsal =** 0 mmol $Cm^{-2}d^{-1}$

Krill (kri): CphLTOkri + CproTOkri + CmicTOkri + CdetTOkri – CkriTOres – CkriTOdet – CkriTOdoc – CkriTOext – *CkriTOmyc – CkriTOpen* = 0 mmol $Cm^{-2}d^{-1}$

Detritus: CphLTOdet + CphSTOdet + CproTOdet + CkriTOdet + CbacTOdet + *CmycTOdet* + *CpenTOdet* + **CsalTOdet** – CdetTOpro – CdetTOmic – CdetTOkri – CdetTOdoc – CdetTOext –

CdetTOsal = 0 mmol $Cm^{-2}d^{-1}$

DOC (doc): CphLTOdoc + CphSTOdoc + CproTOdoc + CmicTOdoc + CkriTOdoc + CbacTOdoc + CdetTOdoc + *CpenTOdoc* + *CmycTOdoc* + **CsalTOdoc** – CdocTObac = 0 mmol $Cm^{-2}d^{-1}$

Penguins (pen): CkriTOpen – CpenTOdet – CpenTOdoc – CpenTOres – CpenTOext = 0 mmol $Cm^{-2}d^{-1}$

Myctophids (myc): CkriTOmyc – CmycTOdet – CmycTOdoc – CmycTOres – CmycTOext = 0 mmol $Cm^{-2}d^{-1}$

Salps (sal) = CphLTOsal + CphSTOsal + CbacTOsal + CproTOsal + CmicTOsal + CdetTOsal – CsalTOres – CsalTOdet – CsalTOdoc – CsalTOext = 0 mmol $Cm^{-2}d^{-1}$

Boundary conditions for WAP 1996 condensed and full carbon models.

Minimum Large Phytoplankton Primary Production: CgpLTOphL – CphLTOres ≥ 59.2 mmol $Cm^{-2}d^{-1}$

Maximum Large Phytoplankton Primary Production: CgpLTOphL – CphLTOres = 280.8 mmol $Cm^{-2}d^{-1}$

Minimum Small Phytoplankton Primary Production: CgpSTOphS – CphSTOres ≥ 29.6 mmol $Cm^{-2}d^{-1}$

Maximum Small Phytoplankton Primary Production: CgpSTOphS – CphSTOres = 140.4 mmol $Cm^{-2}d^{-1}$

Minimum Export: CdetTOext = 5.97 mmol $Cm^{-2}d^{-1}$

Maximum Export : CdetTOext ≥ 17.91 mmol $Cm^{-2}d^{-1}$

Boundary conditions for WAP 1999 carbon model.

Minimum Large Phytoplankton Primary Production: CgpLTOphL – CphLTOres ≥ 5.1 mmol $Cm^{-2}d^{-1}$

Maximum Large Phytoplankton Primary Production: CgpLTOphL – CphLTOres = 34.9 mmol $Cm^{-2}d^{-1}$

Minimum Small Phytoplankton Primary Production: CgpSTOphS – CphSTOres ≥ 2.6 mmol $Cm^{-2}d^{-1}$

Maximum Small Phytoplankton Primary Production: CgpSTOphS – CphSTOres = 17.4 mmol $Cm^{-2}d^{-1}$

Minimum Export: CdetTOext = 1.8 mmol $Cm^{-2}d^{-1}$

Maximum Export : CdetTOext ≥ 5.4 mmol $Cm^{-2}d^{-1}$

Observation equations for WAP 1996 condensed and full carbon models.
Minimum Microzooplankton Grazing: CphLTOmic + CphSTOpro + CphSTOmic ≥ 0 mmol $Cm^{-2}d^{-1}$

Maximum Microzooplankton Grazing: CphLTOmic + CphSTOpro + CphSTOmic = 191.3 mmol $Cm^{-2}d^{-1}$

Minimum Krill Grazing: CphLTOkri ≥ 37.1 mmol $Cm^{-2}d^{-1}$

Maximum Krill Grazing: CphLTOkri = 400.2 mmol $Cm^{-2}d^{-1}$

Minimum Bacterial Production: CbacTOpro + CbacTOmic + CbacTOdet ≥ 0 mmol $Cm^{-2}d^{-1}$

Maximum Bacterial Production: CbacTOpro + CbacTOmic + CbacTOdet = 127.5 mmol $Cm^{-2}d^{-1}$

Minimum Penguin Feeding: CkriTOpen ≥ 0.035 mmol $Cm^{-2}d^{-1}$

Maximum Penguin Feeding: CkriTOpen = 0.105 mmol $Cm^{-2}d^{-1}$

Minimum Myctophid Feeding: CkriTOmyc ≥ 0.060 mmol $Cm^{-2}d^{-1}$

Maximum Myctophid Feeding: CkriTOmyc = 1.08 mmol $Cm^{-2}d^{-1}$

Observation equations for WAP 1999 carbon model.

Minimum Microzooplankton Grazing: CphLTOmic + CphSTOpro + CphSTOmic ≥ 0 mmol $Cm^{-2}d^{-1}$

Maximum Microzooplankton Grazing: CphLTOmic + CphSTOpro + CphSTOmic = 22.5 mmol $Cm^{-2}d^{-1}$

Minimum Krill Grazing: CphLTOkri ≥ 0.1 mmol $Cm^{-2}d^{-1}$

Maximum Krill Grazing: CphLTOkri = 3.0 mmol $Cm^{-2}d^{-1}$
Minimum Bacterial Production: CbacTOpro + CbacTOmic + CbacTOsal + CbacTOdet ≥ 0 mmol $Cm^{-2}d^{-1}$

Maximum Bacterial Production: CbacTOpro + CbacTOmic + CbacTOsal + CbacTOdet = 15 mmol $Cm^{-2}d^{-1}$

Minimum Penguin Feeding: CkriTOpen ≥ 0.01 mmol $Cm^{-2}d^{-1}$

Maximum Penguin Feeding: CkriTOpen = 0.03 mmol $Cm^{-2}d^{-1}$

Minimum Myctophid Feeding: CkriTOmyc ≥ 0.06 mmol $Cm^{-2}d^{-1}$

Maximum Myctophid Feeding: CkriTOmyc = 1.08 mmol $Cm^{-2}d^{-1}$

Salp Minimum Grazing: CphLTOsal ≥ 0.06 mmol $Cm^{-2}d^{-1}$

Salp Maximum Grazing: CphSTOsal = 0.61 mmol $Cm^{-2}d^{-1}$

Appendix B. Biological constraints for inverse models.

Where constraints are different between the WAP and NABE models, the components are listed separately. The temperature, T is equal to 15º C for NABE and -2º C for the WAP. Mbac = pmols of C/bacteria cell, Cbacteria = biomass of bacteria in mmols C m^{-2}, MicC = pmols of C/microzooplankton cell, Cmicro = biomass of microzooplankton in mmols C m^{-2}, MesC = pmols of C/individual, Cmesozoo = biomass of mesozooplankton in mmols C m^{-2}. KrillC = pmols of C/individual, Ckrill = biomass of mesozooplankton in mmols C m^{-2}. MycC = pmols of C/individual myctophid, Cmyc = biomass of myctophids in mmols C m^{-2}.

Biological Constraints	Lower Bound	Upper Bound	Reference
Respiration			
Bacteria	20 % of consumption of DOC	(1.7*(Mbac)^-0.25*EXP(0.0693*(T-20)))*Cbacteria	1,2
Large Phytoplankton	5 % of GPP	30 % of gross primary production	2
Small Phytoplankton	5 % of GPP	30 % of gross primary production	2
Protozoa	20 % of total C intake	None	2
Microzooplankton (NABE)	20 % of total C intake	(14*('MicC')^-0.25*EXP(0.0693*(T-20)))*'Cmicro'	1,2
Micro zooplankton (WAP)	20 % of total C intake	None	1,2
Mesozooplankton (NABE)	20 % of total C intake	(14*(mesoC)^-0.25*EXP(0.0693*(T-20)))*Cmeso	1,2
Krill (WAP)	20 % of total C intake	(14*(krillC)^-0.25*EXP(0.0693*(T-20)))*Ckrill	1,2
Myctophids (WAP)	20 % of total C intake	(14*(mycC)^-0.25*EXP(0.0693*(T-20)))*Cmyc	1,2
Salps (WAP)	20 % of total C intake	(None)	2
Adelies (WAP)	20 % of total C intake	(None)	2
Excretion			
Large Phytoplankton	2 % of large phytoplankton NPP	55 % of large phytoplankton NPP	3
Small Phytoplankton	2 % of small phytoplankton NPP	55 % of small phytoplankton NPP	3
Protozoa	10 % of total C intake	100 % of protozoan respiration	4
Microzooplankton	10 % of total C intake	100 % of microzooplankton respiration	4
Mesozooplankton (NABE)	10 % of total C intake	100 % of mesozooplankton respiration	4
Krill (WAP)	10 % of total C intake	100 % of krill respiration	4
Myctophids (WAP)	10 % of total C intake	100 % of myctophid respiration	4
Salps (WAP)	10 % of total C intake	100 % of salp respiration	4
Adelies (WAP)	10 % of total C intake	100 % of adelie respiration	4

Biological Constraints Continued	Lower Bound	Upper Bound	Reference
Assimilation efficiency			
Protozoa	C output to Detritus <= 50% of total C intake	C output to Detritus >= 10% of total C intake	2
Microzooplankton	C output to Detritus <= 50% of total C intake	C output to Detritus >= 10% of total C intake	2
Mesozooplankton (NABE)	C output to Detritus <= 50% of total C intake	C output to Detritus >= 10% of total C intake	2
Krill (WAP)	C output to Detritus <= 28% of total C intake	C output to Detritus >= 6% of total C intake	6
Myctophids (WAP)	C output to Detritus <= 50% of total C intake	C output to Detritus >= 10% of total C intake	2
Adelies (WAP)	C output to Detritus <= 50% of total C intake	C output to Detritus >= 10% of total C intake	2,5
Salps (WAP)	C output to Detritus <= 50% of total C intake	C output to Detritus >= 30% of total C intake	2,7
Net production efficiency			
Bacteria	bacteria to DOC + bacterial respiration <= 95% DOC to bacteria	bacteria to DOC + bacterial respiration >= 50% DOC to bacteria	2
Gross production efficiency			
Protozoa	losses to respiration + detritus + DOC <= 90 % of total carbon intake	losses to respiration + detritus + DOC >= 60 % of total carbon intake	2
Microzooplankton	losses to respiration + detritus + DOC <= 90 % of total carbon intake	losses to respiration + detritus + DOC >= 60 % of total carbon intake	2
Mesozooplankton (NABE)	losses to respiration + detritus + DOC <= 90 % of total carbon intake	losses to respiration + detritus + DOC >= 60 % of total carbon intake	
Krill (WAP)	losses to respiration + detritus + DOC <= 90 % of total carbon intake	losses to respiration + detritus + DOC >= 60 % of total carbon intake	2
Myctophids (WAP)	losses to respiration + detritus + DOC <= 90 % of total carbon intake	losses to respiration + detritus + DOC >= 60 % of total carbon intake	2
Adelies (WAP)	losses to respiration + detritus + DOC <= 90 % of total carbon intake	losses to respiration + detritus + DOC >= 60 % of total carbon intake	2
Salps (WAP)	Losses to respiration + detritus + DOC <= 90 % of total carbon intake	losses to respiration + detritus + DOC >= 60 % of total carbon intake	2
Ingestion			
Bacteria	None	(3.6*(Mbac)^-0.25*EXP(0.0693*(T-20)))*Cbacteria	1,2
Mesozooplankton (NABE)	None	(63*(mesC)^-0.25*EXP(0.0693*(T-20)))*Cmesozoo	1,2
Krill (WAP)	None	(63*(krill C)^-0.25*EXP(0.0693*(T-20)))*Ckrill	1,2

References. 1. Moloney & Field (1989) 2. Vezina & Platt (1989) 3. Baines and Pace (1991)

4. Vezina and Pace (1994) 5. Salihoglu, Fraser and Hoffman (2001) 6. Kato (1982) 7. Perisonotto and Pakhomov (1998)

References Cited

Baines, S.B., Pace, M.L., 1991. The production of dissolved organic matter by phytoplankton and its importance to bacteria: patterns across marine and freshwater systems. Limnology and Oceanography 36, 1078-1090.

Becquevort, S., 1995. Nanoprotozooplankton in the Atlantic sector of the Southern Ocean during early spring: biomass and feeding activities. Deep Sea Research II 44 (1-2), 355-373.

Buessler, K.O., Bacon, M.P., Cochran, J.K., Livingston, H.D., 1992. Carbon and nitrogen export during the JGOFS North Atlantic bloom experiment estimated from 234Th: 238U disequilibria. Deep Sea Research II 39, 1115-1137.

Carlson, C.A., Ducklow, H.W., Michaels, A.F., 1994. Annual flux of dissolved organic carbon from the euphotic zone in the northwestern Sargasso Sea. Nature 371 (6496), 405-408.

Culik, B.M., Wilson, R.P., 1991. Energetics of underwater swimming in Adélie penguins. Journal of Comparitive Physiology 161 (3), 285-291.

Dam, H., CA Miller, and SH Jonasdottir, 1993. The trophic role of mesozooplankton at 47°N, 20°W during the North Atlantic Bloom Experiment. Deep Sea Research II 40 (1-2), 197-212.

Dam, H.G., X. Zhang, M. Butler, and M.R. Roman, 1995. Mesozooplankton grazing and metabolism at the equator in the central Pacific: Implications for carbon and nitrogen fluxes. Deep Sea Research 42 (2-3), 735-756.

Daniels, R.M., 2003. Inverse model analysis of plankton food webs in the north Atlantic and western Antarctic Peninsula. Master's Thesis, College of William and Mary, Virginia Institute of Marine Science, Gloucester Point, 1-178.

Donali, E., Olli, K., Heiskanen, A.S., Andersen, T., 1998. Carbon flow patterns in the planktonic food web of the Gulf of Riga, the Baltic Sea: a reconstruction by the inverse method. Journal of Marine Systems 23, 251-268.

Ducklow, H.W., 2003. Chapter 1. Biogeochemical Provinces: Towards a JGOFS Synthesis. In: Fasham, M.J.R. (Ed.s), Ocean Biogeochemistry: A New Paradigm. Springer-Verlag, New York, pp. 3-18.

Ducklow, H.W., Fasham, M.J.R., Vezina, A.F., 1989. Derivation and analysis of flow networks for oceanic plankton systems. In: Wulff, F., Field, J.G., Mann, K.H. (Ed.s), Network Analysis in Marine Ecology. Springer-Verlag, Berlin, pp. 159-205.

Ducklow, H.W., Harris, R., 1993. Introduction to the JGOFS North Atlantic bloom study. Deep-Sea Research II 40 (1-2), 1-8.

Ducklow, H.W., Harris, R.P., 1993. Introduction to the JGOFS North Atlantic bloom experiment. Deep Sea Research Part II: Topical Studies in Oceanography 40 (1-2), 1-8.

Ducklow, H.W., Kirchman, D.L., Quinby, H.L., Carlson, C.A., Dam, H.G., 1993. Stocks and dynamics of bacterioplankton carbon during the spring phytoplankton bloom in the eastern North Atlantic Ocean. Deep-Sea Research II 40 (1-2), 245-63.

Dugdale, R.C., Goering, J.J., 1967. Uptake of new and regenerated forms of nitrogen in primary production. Limnology and Oceanography 12 (2), 196-206.

Eldridge, P.M., Jackson, G.A., 1993. Benthic trophic dynamics in California coastal basin and

continental slope communities inferred using inverse analysis. Marine Ecology Progress Series 99 (1-2), 115-135.

Eppley, R.W., Peterson, B.J., 1979. Particulate organic matter flux and planktonic new production in the deep ocean. Nature 282 (5740), 677-680.

Fasham, M.J.R., 1995. Variations in the seasonal cycle of biological production in subarctic oceans: A model sensitivity analysis. Deep-Sea Res. 42 (7), 1111-1149.

Fuhrman, J.A., Sleeter, T., Carlson, C.A., Proctor, L.M., 1989. Dominance of bacterial biomass in the Sargasso Sea and its ecological implications. Marine Ecology Progress Series 57 (3), 207-217.

Froneman, P., and R. Perissinotto, 1996. Microzooplankton grazing in the Southern Ocean: implications for the carbon cycle. P.S.Z.N.I.: Marine Ecology 17 (1-3), 99-115.

Garibotti, I.A., Ferrario, M.E., Smith, R.C., Ross, R.M., Quetin, L.B., Vernet, M., 2001. Marine phytoplankton community structure and spatial distribution west of the Antarctic Peninsula, January 1997 (submitted). Aquatic Microbial Ecology.

Garrison, D.L., Gowing, M.M., Hughes, M.P., Campbell, L., Caron, D.A., Dennett, M.R., Shalapyonok, L., Olson, R.J., Landry, M.L., Brown, S.L., Liu, H.-B., Azam, F., Steward, G., Ducklow, H.W., Smith, D.C., 2000. Microbial food web structure in the Arabian Sea: A U. S. JGOFS Study. Deep-Sea Research II 47 1387-1422.

Garside, C., and J. Garside, 1993. The "f-ratio" on 20W during the North Atlantic Bloom Experiment. Deep-Sea Res II 40 (1-2), 75-90.

Harrison, W.G., Head, E.J.H., Horne, E.P.W., Irwin, B., Li, W.K.W., Longhurst, A.R., Paranjape, M.A., Platt, T., 1993. The western North Atlantic bloom experiment. Deep Sea Research Part II: 40 (1-2), 279-305.

Holm-Hansen, O., Mitchell, B.G., 1991. Spatial and temporal distribution of phytoplankton and primary production in the western Bransfield Strait region. Deep-Sea Research 38 (8-9), 961-980.

Huntley, M.E., Lopez, M.D.G., Karl, D.M., 1991. Top predators in the Southern Ocean: A Major Leak in the Biological Carbon Pump. Science 253 64-66.

Jackson, G., and PM Eldridge, 1992. Food web analysis of a planktonic system off Southern California. Progress in Oceanography 30 (1-4), 223-251.

Karl, D.M., 1999a. A sea of change: Biogeochemical variability in the North Pacific subtropical gyre. Ecosystems 2 (3), 181-214.

Karl, D.M., 1999b. Uncoupling of bacteria and phytoplankton during the austral spring bloom in Gerlache Strait. Antarctic Peninsula. *Aquatic Microbial Ecology*, 19, 13-27.

Karl, D.M., Christian, J.R., Dore, J.E., Letelier, R.M., 1996. Microbiological oceanography in the region west of the Antarctic Peninsula: Microbial dynamics, nitrogen cycle and carbon flux. In: Ross, R.M., Hofmann, E.E., Quetin, L.B. (Ed.s), Foundations for ecological research west of the Antarctic Peninsula. American Geophysical Union, Washington, DC, pp. 303-332.

Lancraft, T.M., Hopkins, T.L., Torres, J.J., Donnelly, J., 1991. Oceanic micronektonic/macrozooplanktonic community structure and feeding in the ice covered Antarctic water during the winter (AMERIEZ 1988). Polar Biology 11, 157-167.

Landry, M.R., Barber, R.T., Bidigare, R.R., Chai, F., Coale, K.H., Dam, H.G., Lewis, M.R., Lindley, S.T., McCarthy, J.J., Roman, M.R., Stoecker, D.K., Verity, P.G., White, J.R., 1997. Iron and grazing constraints on primary production in the central equatorial Pacific: an EqPac synthesis. Limnology and Oceanography 42 (3), 405-418.

Lascara, C.M., Hofmann, E.E., Ross, R.M., Quetin, L.B., 1999. Seasonal variability in the distribution of Antarctic krill, Euphausia superba, west of the Antarctic Peninsula. Deep-Sea Research 46 (6), 951-984.

Legendre, L., Gosselin, M., 1989. New production and export of organic matter to the deep ocean: consequences of some recent discoveries. Limnology and Oceanography 34 (7), 1374-1380.

Legendre, L., Rassoulzadegan, F., 1996. Food-web mediated export of biogenic carbon in oceans: hydrodynamic control. Marine Ecology Progress Series 145 (1-3), 179-193.

Lochte, K., Ducklow, H.W., Fasham, M.J.R., Stienen, C., 1993. Plankton succession and carbon cycling at 47º N 20º W during the JGOFS North Atlantic Bloom Experiment. Deep-Sea Research II 40 (1-2), 91-114.

Longhurst, A., 1995. Seasonal cycles of pelagic production and consumption. Progress in Oceanography 36 (2), 77-167.

Martin, J.H., Fitzwater, S.E., Gordon, R.M., Hunter, C.N., Tanner, S.J., 1993. Iron, primary production and carbon-nitrogen flux studies during the JGOFS North Atlantic Bloom Experiment. Deep-Sea Research II 40 (1-2), 115-134.

Martin, J.H., Knauer, G.A., Karl, D.M., Broenkow, W.W., 1987. VERTEX: Carbon cycling in the Northeast Pacific. Deep-Sea Research 34 (2A), 267-285.

Michaels, A.F., Silver, M.W., 1988. Primary production, sinking fluxes and the microbial food web. Deep-Sea Research 35, 473-490.

McCarthy, J.J., Garside, C., Nevins, J.L., Barber, R.T., 1996. New production along 140º W in the Equatorial Pacific during and following the 1992 El Nino event. Deep-Sea Research II 43 (4-6), 1065-1093.

Moloney, C.L., and J. G. Field, 1989. General allometric equations for rates of nutrient uptake, ingestion, and respiration in plankton organisms. Limnology and Oceanography 34 (7), 1290-1299.

Niquil, N., Jackson, J.B.C., Legendre, L., Dellesalle, B., 1998. Inverse model analysis of the planktonic food web of Takapoto Atoll (French Polynesia). Marine Ecology Progress Series 165 17-29.

P.M., E., Jackson, G.A., 1993. Benthic trophic dynamics in California coastal basin and continental slope communities inferred using inverse analysis. Marine Ecology Progress Series 99 115-135.

Pakhomov, E.A., Perissinotto, R., McQuaid, C.D., 1996. Prey composition and daily rations of myctophid fishes in the Southern Ocean. Marine Ecology Progress Series 134 (1-3), 1-14.

Parker, R.L., 1977. Understanding inverse theory. Annual Review of Earth Planetary Science 5, 35-64.

Pauly, D., Christensen, V., Walters, C., 2000. Ecopath, ecosim, and ecospace as tools for evaluating ecosystem impact of fisheries. ICES Journal of Marine Science 57 (3), 697-706.

Perissinotto, R., A. Pakhomov, E., 1998. The trophic role of the tunicate Salpa thompsoni in the Antarctic marine ecosystem. Journal of Marine Systems 17 (1-4), 361-374.

Pesant, S., Legendre, L., Gosselin, M., Ashjian, C., Booth, B., Daly, K., Fortier, L., Hirche, H.J., Michaud, J., Smith, R.E.H., Smith, S., Smith, W.O., Jr., 1998. Pathways of carbon cycling in the euphotic zone: the fate of large-sized phytoplankton in the Northeast Water Polynya. Journal of Plankton Research 20 (7), 1267-1291.

Pomeroy, L.R., 2001. Caught in the food web: complexity made simple? Scientia Marina 65 (Suppl. 2), 31-40.

Richardson, T.L., Ducklow, H.W., Jackson, G.A., Roman, M.R., 2004. Planktonic food webs of the equatorial Pacific at 140°W: a synthesis of EqPac time-series carbon flux data. Deep Sea Research (in press).

Rivkin, R.B., Legendre, L., Deibel, D., Tremblay, J.E., Klein, B., Crocker, K., Roy, S., Silverberg, N., Lovejoy, C., Mesplé, F., Romero, N., Anderson, M.R., Matthews, P., Savenkoff, C., Vézina, A., Therriault, J.C., Wesson, J., Bérubé, C., Ingram, R.G. Vertical flux of biogenic carbon in the ocean: is there food web control? Science 272 (5265), 1163-1166.

Ross, R.M., Quetin, L.B., Lascara, C.M., 1996. Distribution of Antarctic krill and dominant zooplankton west of the Antarctic Peninsula. In: Ross, R.M., Hofmann, E.E., Quetin, L.B. (Ed.s), Foundations for ecological research west of the Antarctic Peninsula. American Geophysical Union, Washington, DC, pp. 199-217.

Ryther, J., 1969. Photosynthesis and fish production in the sea. Science 166, 72-76.

Salihoglu, B., Fraser, W.R., Hofmann, E.E., 2001. Factors affecting fledging weight of Adelie penguin (Pygoscelis adeliae) chicks: a modeling study. Polar Biology 24 (5), 328-337.

Smith, R.C., Baker, K.S., Byers, M.L., Stammerjohn, S.E., 1998. Primary Productivity of the Palmer Long Term Ecological Research Area and the Southern Ocean. Journal of Marine Systems 17 (1-4), 245-259.

Ulanowicz, R.E., 1986. NETWRK3: A package of computer algorithms to analyze ecological flow networks, pascal implementation for the IBM-PC. University of Maryland Center for Environmental & Estuarine Studies, Solomons, MD.

Verity, P.G., Stoecker, D.K., Sieracki, M.E., Nelson, J.R., 1993. Grazing, growth and mortality of microzooplankton during the 1989 North Atlantic spring bloom at 47º N, 18º W. Deep-Sea Research 40 (9), 1793-1814.

Vezina, A.F., Pace, M.L., 1994. An inverse model analysis of planktonic food webs in experimental lakes. Canadian Journal of Fisheries and Aquatic Sciences 51 (9), 2034-2044.

Vézina, A.F., Pahlow, M ., 2003. Reconstruction of ecosystem flows using inverse methods: how well do they work? Journal of Marine Systems 40-41, 55-77.

Vezina, A.F., Platt, T., 1988. Food web dynamics in the ocean. I. Best-estimates of flow networks using inverse methods. Marine Ecology Progress Series 42, 269-287.

Watson, A.J., Whitfield, M., 1985. Composition of particles in the global ocean. Deep-Sea Research 32 (9A), 1023-1039.

Wunsch, C., 1978. The north Atlantic general circulation west of 50ºW determined by inverse methods. Review of Geophysics and Space Physics 16, 583-620.

Wunsch, C., Minster, J.F., 1982. Methods for box models and ocean circulation tracers: mathematical programming and nonlinear inverse theory. Journal of Geophysical Research 87, 5647-5662.

Figure Captions

Figure 1. General ocean food web inverse model. Inputs are from gross primay production for small phytoplankton (gpS) and large phytoplankton (gpL). Gray flows leaving compartments are losses to respiration. Export from the surface ocean enters the ext compartment. Width of arrow is proportional to the magnitude of the flow.

Figure 2. Living components in the modeled western Antarctic Peninsula Food Web for January, 1996 and January, 1999. Short food web flows that lead to export from the surface ocean and microbial food web flows that lead to recycling within the food web are highlighted. Arrows leaving krill and salps without entering another compartment represent export of faecal pellets and are components of the short food web.

Figure 3. NABE measurements at 47º N 20º W during May, 1989 aboard the Atlantis II. Primary production (**a**), phytoplankton biomass (**b**), bacterial production (**c**), bacterial biomass (**d**), microzooplantkon grazing (**e**), microzooplankton biomass (**f**), mesozooplankton grazing (**g**), mesozooplankton biomass (**h**). ND = No data measurement taken on that day.

Figure 4. Adélie penguin foraging areas for 1996 and 1999 within the Palmer LTER regional grid that is sampled during the annual January cruise. The grid lines are every 100 kms along the coast of the western Antarctic Peninsula, and the stations are every 20 kms along a grid line, extending 200 kms offshore (Smith et al., 1995). The foraging areas are centered at Palmer Station on Anvers Island. The hashed area within the circles represents the 1/3 of the circle that mainly lies over land and was excluded in the calculation of the penguin foraging areas. Measurements at stations within the foraging areas were averaged and used as inputs to the models.

Figure 5. WAP measurements from Palmer Station near shore stations B, E, and Le Maire and from the January regional cruises, including primary production for 1996 (**a**) and 1999 (**d**), phytoplankton biomass for 1996 (**b**) and 1999 (**e**) and bacterial biomass for 1996 (**c**) and 1999 (**f**). For the regional grid stations, the first 3 numbers is the grid line along shore and the last 3 after the "." is the number of km offshore. For example station, 600.100 is on the 600 grid line and is 100 km offshore and 600.035 is on the 600 grid line and 35 km offshore.

Figure 6. (a) NABE carbon inverse solution and (b)simplified WAP 1996 carbon inverse solution. The myctophids and penguins were excluded from the WAP model for a direct comparison with the NABE carbon model. Width of the flow is proportional to the magnitude of the flow. Grey flows leaving compartments are losses to respiration. Inputs are from gross primary production for small phytoplankton (gps) and large phytoplankton (gpl). Export from the surface ocean enters the ext compartment. Black arrows are flows that were zero in the inverse solution.

Figure 7. WAP inverse solution food web graphs for 1996(**a**) and 1999(**b**).Width of the flow is proportional to the magnitude of the flow. Grey flows leaving compartments are losses

to respiration. Inputs are from gross primary production for small phytoplankton (gps) and large phytoplankton (gpl). Export from the surface ocean enters the ext compartment. Black arrows are flows that were zero in the inverse solution.

Figure 8. Contributions to the DOC pools in (a) the NABE carbon inverse solution and (b) the 1996 WAP carbon inverse solution, as a % of the total flows entering.

Table 1 Data input to the North Atlantic Bloom Experiment (NABE) and the western Antarctic Peninsula (WAP) models. NABE entries represent statistics for the May 18-31, 1989 time series (Figure 3). WAP entries are for all January observations within the Adélie penguin foraging territory for 1996 and 1999 (see text for details)

	NABE 1989				**WAP 1996**				**WAP 1999**			
	AVG	**St Dev**	**Min**	**Max**	**AVG**	**St Dev**	**Min**	**Max**	**AVG**	**St Dev**	**Min**	**Max**
Phyto-plankton Production (mmol C $m^{-2}d^{-1}$)	88	25	63	113	254	166	88	420	29	22	7	52
Small Phyto-plankton Production (mmol C $m^{-2}d^{-1}$)	44	13	32	57	85	55	29	140	10	7	3	17
Large Phyto-plankton Production (mmol C $m^{-2}d^{-1}$)	44	13	32	57	170	111	59	281	20	15	5	35
Phyto-plankton Biomass (mmol C m^{-2})	423	111	–	–	1438	1008	–	–	137	82	54	219
Bacterial Productivity (mmol C $m^{-2}d^{-1}$)	20	6	13	26	–	–	0	50 % of PP	–	–	0	50 % of PP
Bacterial biomass (mmol C m^{-2})	86	33	–	–	10	6	–	–	3	1	–	–
Microzoo-Plankton Grazing (mmol C $m^{-2}d^{-1}$)	81	–	41	122	–	–	0	75 % of PP	–	–	0	75 % of PP
Microzoo-plankton Biomass (mmol C m^{-2})	91	46	–	–	–	–	–	–	–	–	–	–
Mesozoo-plankton Grazing (mmol C $m^{-2}d^{-1}$)	2	–	3	1	–	–	37	400		–	0.1	3

Table 1 (continued)

	NABE 1989				WAP 1996				WAP 1999			
	AVG	**St Dev**	**Min**	**Max**	**AVG**	**St Dev**	**Min**	**Max**	**AVG**	**St Dev**	**Min**	**Max**
Krill Biomass (mmol C m^{-2})	7	6	–	–	226	–	–	–	0.2	–	–	–
Mesozoo-plankton Biomass (mmol C m^{-2})	7	6	–	–	2672	–	–	–	302	–	–	–
Export (mmol C $m^{-2}d^{-1}$)	16	–	8	24	12	–	6	18	4	–	2	5
Adelie Grazing (mmol C $m^{-2}d^{-1}$)	–	–	–	–	0.07	–	0.03	0.10	0.02	–	0.01	0.02
Myctophid Grazing (mmol C $m^{-2}d^{-1}$)	–	–	–	–	–	–	0.06	1.08	–	–	0.06	1.08
Myctophid Biomass (mmol C m^{-2})	–	–	–	–	0.73	–	–	–	0.73	–	–	–
Salp Grazing (mmol C $m^{-2}d^{-1}$)	–	–	–	–	–	–	–	–	–	–	0.06	0.61

Table 2 Comparison of the North Atlantic carbon inverse solution and the 1996 western Antarctic Peninsula simplified carbon solution

Flow #	Food Web Flow again, font changed	WAP96 Flows (mmol $Cm^{-2}d^{-1}$)	NABE Flows (mmol $Cm^{-2}d^{-1}$)	WAP96 Flows (% of PP)	NABE Flows (% of PP)
1	Large phytoplankton gross primary production	62.3	33.2	70	53
2	Large phytoplankton respiration	3.1	1.7	4	3
3	Microzooplankton grazing of large phytoplankton	9.8	15.2	11	24
4	Krill or mesozooplankton grazing of large phytoplankton	37.1	3.5	42	6
5	Large phytoplankton to detritus	8.9	4.3	10	7
6	Large phytoplankton release of DOC	3.4	8.5	4	14
7	Small phytoplankton gross primary production	31.2	33.2	35	53
8	Small phytoplankton respiration	1.6	1.7	2	3
9	Protozoan grazing of small phytoplankton	11.5	13.4	13	21
10	Microzooplankton grazing of small phytoplankton	8.7	11.9	10	19
11	Small phytoplankton to detritus	7.7	1.0	9	2
12	Small phytoplankton release of DOC	1.7	5.2	2	8
13	Microzooplankton consumption of protozoans	1.3	0.5	2	1
14	Krill or mesozooplankton consumption of protozoans	0.2	1.2	0	2
15	Protozoan respiration	11.1	10.1	12	16
16	Protozoans to detritus	1.6	1.7	2	3
17	Protozoans to DOC	1.6	3.8	2	6
18	Microzooplankton respiration	14.6	11.9	16	19
19	Krill or mesozooplankton consumption of microzooplankton	2.1	0.5	2	1
20	Microzooplankton to detritus	2.1	3.0	2	5
21	Microzooplankton to DOC	2.1	5.6	2	9
22	Krill or mesozooplankton respiration	17.3	1.2	20	2
23	Krill or mesozooplankton to detritus (Fecal pellets)	2.4	0.8	3	1

Table 2 (continued)

Flow #	Food Web Flow	WAP Flows (mmol $Cm^{-2}d^{-1}$)	NABE Flows (mmol $Cm^{-2}d^{-1}$)	WAP 1996 Flows (% of PP)	NABE Flows (% of PP)
24	Krill or mesozooplankton to DOC	3.9	1.2	4	2
25	Bacterial respiration	12.1	11.6	14	18
26	Bacteria to protozoans	0.6	4.0	1	6
27	Bacteria to microzooplankton	0.0	2.6	0	4
28	Bacteria to detritus	0.0	4.0	0	6
29	Bacteria to DOC	0.0	5.4	0	8
30	Protozoan consumption of detritus	3.7	0.0	4	0
31	Microzooplankton consumption of detritus	1.0	0.0	1	0
32	Krill or mesozooplankton consumption of detritus	0.0	0.0	0	0
33	Detritus to DOC	0.0	4.3	0	7
34	Bacterial ingestion of DOC	12.7	34.0	14	54
35	Total Particulate Export out of the top 35 m	17.9	10.6	20	17
36	Krill or mesozooplankton to export (Consumption by higher trophic levels or mortality)	15.8	2.1	18	3

Table 3 Western Antarctic Peninsula (WAP) 1996 and 1999 carbon inverse solution flows

Flow #	Flow	WAP 1996 Flows (mmol C $m^{-2}d^{-1}$)	WAP 1999 Flows (mmol C $m^{-2}d^{-1}$)	WAP 1996 Flows (% of PP)	WAP 1999 Flows (% of PP)
1	Large phytoplankton gross primary production	62.3	5.4	70.2	70.1
2	Large phytoplankton respiration	3.1	0.3	3.5	3.5
3	Microzooplankton grazing of large phytoplankton	9.8	1.3	11.1	16.5
4	Krill grazing of large phytoplankton	37.1	1.6	41.8	21.1
5	Large phytoplankton to detritus	8.9	1.2	10.0	16.2
6	Large phytoplankton release of DOC	3.4	0.4	3.8	5.2
7	Small phytoplankton gross primary production	31.2	2.7	35.1	35.1
8	Small phytoplankton respiration	1.6	0.1	1.8	1.8
9	Protozoan grazing of small phytoplankton	11.4	1.0	12.9	12.4
10	Microzooplankton grazing of small phytoplankton	8.7	0.7	9.8	9.2
11	Small phytoplankton to detritus	7.7	0.7	8.7	8.9
12	Small phytoplankton release of DOC	1.7	0.2	1.9	2.6
13	Microzooplankton consumption of protozoans	1.2	0.0	1.4	0.0
14	Krill consumption of protozoans	0.4	0.0	0.4	0.3
15	Protozoan respiration	11.0	0.9	12.4	11.3
16	Protozoans to detritus	1.6	0.1	1.8	1.6
17	Protozoans to DOC	1.6	0.1	1.8	1.6
18	Microzooplankton respiration	14.5	1.2	16.4	15.4
19	Mesozooplantkton consumption of microzooplankton	2.1	0.2	2.3	2.2
20	Microzooplankton to detritus	2.1	0.2	2.3	2.6
21	Microzooplankton to DOC	2.1	0.2	2.3	2.6
22	Krill respiration	17.5	1.0	19.7	12.5
23	Krill to detritus (Fecal pellets)	2.4	0.1	2.7	1.7
24	Krill to DOC	4.0	0.2	4.5	2.9
25	Bacterial respiration	12.2	1.1	13.7	14.7
26	Bacteria to protozoans	0.6	0.0	0.7	0.1

Table 3 (continued)

Flow #	Flows	WAP 1996 Flows (mmol C $m^{-2}d^{-1}$)	WAP 1999 Flows (mmol C $m^{-2}d^{-1}$)	WAP 1996 Flows (% of PP)	WAP 1999 Flows (% of PP)
27	Bacteria to microzooplankton	0.0	0.0	0.0	0.0
28	Bacteria to detritus	0.0	0.0	0.0	0.0
29	Bacteria to DOC	0.0	0.0	0.0	0.0
30	Protozoan consumption of detritus	3.7	0.3	4.2	3.6
31	Microzooplankton consumption of detritus	1.0	0.0	1.1	0.3
32	Krill consumption of detritus	0.1	0.4	0.2	4.9
33	Detritus to DOC	0.0	0.0	0.0	0.0
34	Bacterial ingestion of DOC	12.8	1.3	14.5	17.3
35	Total particulate export out of the top 35 m	17.8	1.4	20.1	18.2
36	Krill to export (Consumption by higher trophic levels or death)	14.7	0.6	16.5	7.6
37	Myctophid consumption of krill	1.1	0.3	1.2	3.4
38	Penguins consumption of krill	0.11	0.03	0.12	0.39
39	Penguins to detritus	0.03	0.01	0.04	0.12
40	Penguins to DOC	0.01	0.00	0.01	0.04
41	Penguin respiration	0.03	0.01	0.04	0.12
42	Penguin to export (Consumption by higher trophic levels or death)	0.03	0.01	0.04	0.12
43	Myctophids to detritus	0.3	0.1	0.4	1.0
44	Myctophids to DOC	0.1	0.0	0.1	0.3
45	Myctophids to respiration	0.3	0.1	0.4	1.0
46	Myctophids to export (Consumption by higher trophic levels or death)	0.3	0.1	0.4	1.0
47	Salp consumption of large phytoplankton	–	0.6	–	7.6
48	Salp consumption of small phytoplankton	–	0.0	–	0.3
49	Salp consumption of bacteria	–	0.2	–	2.5
50	Salp consumption of protozoans	–	0.1	–	1.3
51	Salp consumption of microzooplankton	–	0.2	–	3.2
52	Salp consumption of detritus	–	0.5	–	6.0
53	Salp respiration	–	0.6	–	8.4
54	Salps to detritus (fecal pellets)	–	0.2	–	2.1
55	Salps to DOC	–	0.2	–	2.1
56	Salps to export	–	0.6	–	8.4

Table 4 Comparison of the microbial and short food web flows for the Western Antarctic Peninsula (WAP) 1996 condensed carbon model and the North Atlantic Bloom Experiment (NABE) carbon model

Microbial Food Web Flows	**WAP 1996 (% of PP)**	**NABE (% of PP)**
S Phytoplankton to Detritus	8.7	1.5
S Phytoplankton to DOC	1.9	8.3
Protozoan Grazing of S Phytoplankton	12.9	21.2
Protozoan Grazing of Bacteria	0.7	6.4
Microzooplankton Grazing of Bacteria	0.0	4.1
Microzooplankton Grazing of L Phytoplankton	11.1	24.1
Microzooplankton Grazing of S Phytoplankton	9.8	18.9
Microzooplankton Grazing of Protozoans	1.5	0.8
Bacterial DOC Ingestion	14.3	54.0
Bacterial Release of DOC	0.0	8.5
Bacteria to Detritus	0.0	6.4
Protozoan to Detritus	1.8	2.8
Protozoans to DOC	1.8	6.1
Microzooplankton to DOC	2.4	8.9
Detritus to DOC	0.0	6.8
Detritus to Protozoans	4.2	0.0
Detritus to Microzooplankton	1.1	0.0
Microzooplankton to Detritus	2.4	4.8
Total	74.5	183.7
Short Food Web Flows		
L Phytoplankton to detritus	10.0	6.8
Krill Grazing of L Phytoplankton	41.8	5.5
Other Krill Production	17.8	3.3
Krill Fecal pellets	2.7	1.3
Total	72.2	16.9
Microbial Food Web Flows / Short Food Web Flows	1.0	10.8

Table 5 Network analysis indices for the Western Antarctic Peninsula 1996 condensed carbon model and the NABE carbon model (see section 4.5)

Index	**WAP 1996**	**NABE**
Fbac (%)	1	23
Fpro (%)	21	40
Fmic (%)	27	48
Fkri or Fmes (%)	52	12
L	1.4	2.2
Total Ingestion / PP	1.0	1.4

Table 6 Effective trophic levels of components in the North Atlantic Bloom Experiment (NABE) carbon model and the western Antarctic Peninsula 1996 condensed carbon model (see section 4.5)

	Effective Trophic Level	
Component	**NABE**	**WAP 1996**
Small Phytoplankton	1	1
Large Phytoplankton	1	1
Protozoans	2.28	2.04
Microzooplankton	2.14	2.06
Mesozooplankton / Krill	2.49	2.07
Bacteria	2	2
DOC	1	1
Detritus	1	1

Table 7 Comparison of food web classifications of the Inverse Model results with the 5 different food web types described by Legendre & Rassoulzadegan (1996) (see section 5.3 for details)

Biogenic carbon pathways	P_L/P_T	**M**	R_T/P_T	F_T/P_T	D_T/P_T
(1) Sinking of ungrazed cells	1.00	0.00	0.00	0.00	1.00
(2) Herbivorous food web	0.80	0.55	0.30	0.60	0.10
(3) Multivorous food web	0.35	0.65	0.60	0.30	0.10
(4) Microbial food web	0.10	0.25 or 0.75	0.80	0.20	0.00
(5) Microbial loop	0.00	0 or 1	1.00	0.00	0.00
Inverse Models					
NABE Carbon	0.50	–	0.90	0.03	0.07
WAP 1996 Carbon	0.67	–	0.63	0.20	0.17
WAP 1999 Carbon	0.67	–	0.68	0.22	0.10

Figure 1

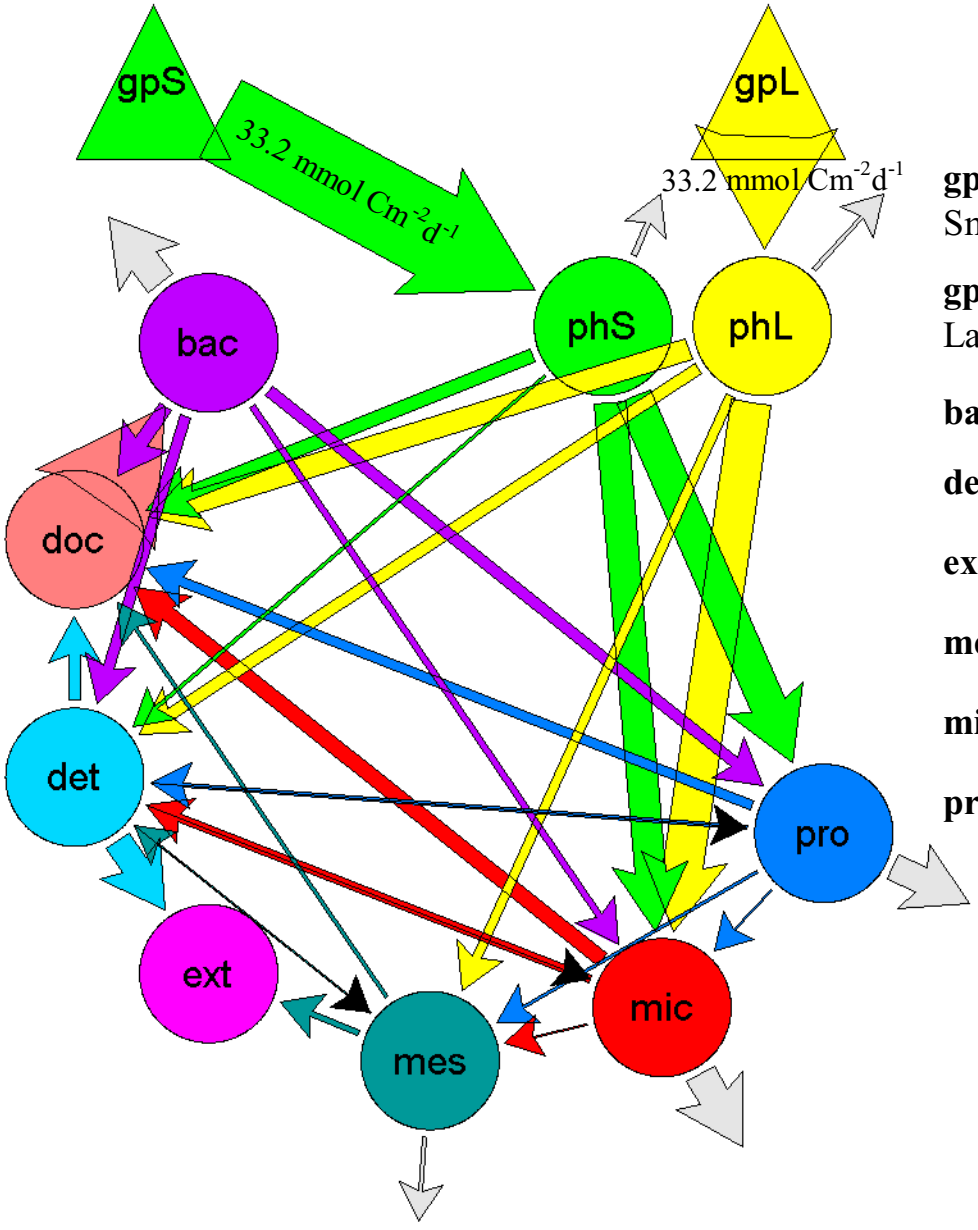

gpS = Gross PP for Small Phytoplankton

gpL = Gross PP for Large Phytoplankton

bac = Bacteria

det = Detritus

ext = External

mes = Mesozooplankton

mic = Microzooplankton

pro = Protozoans

Figure 2

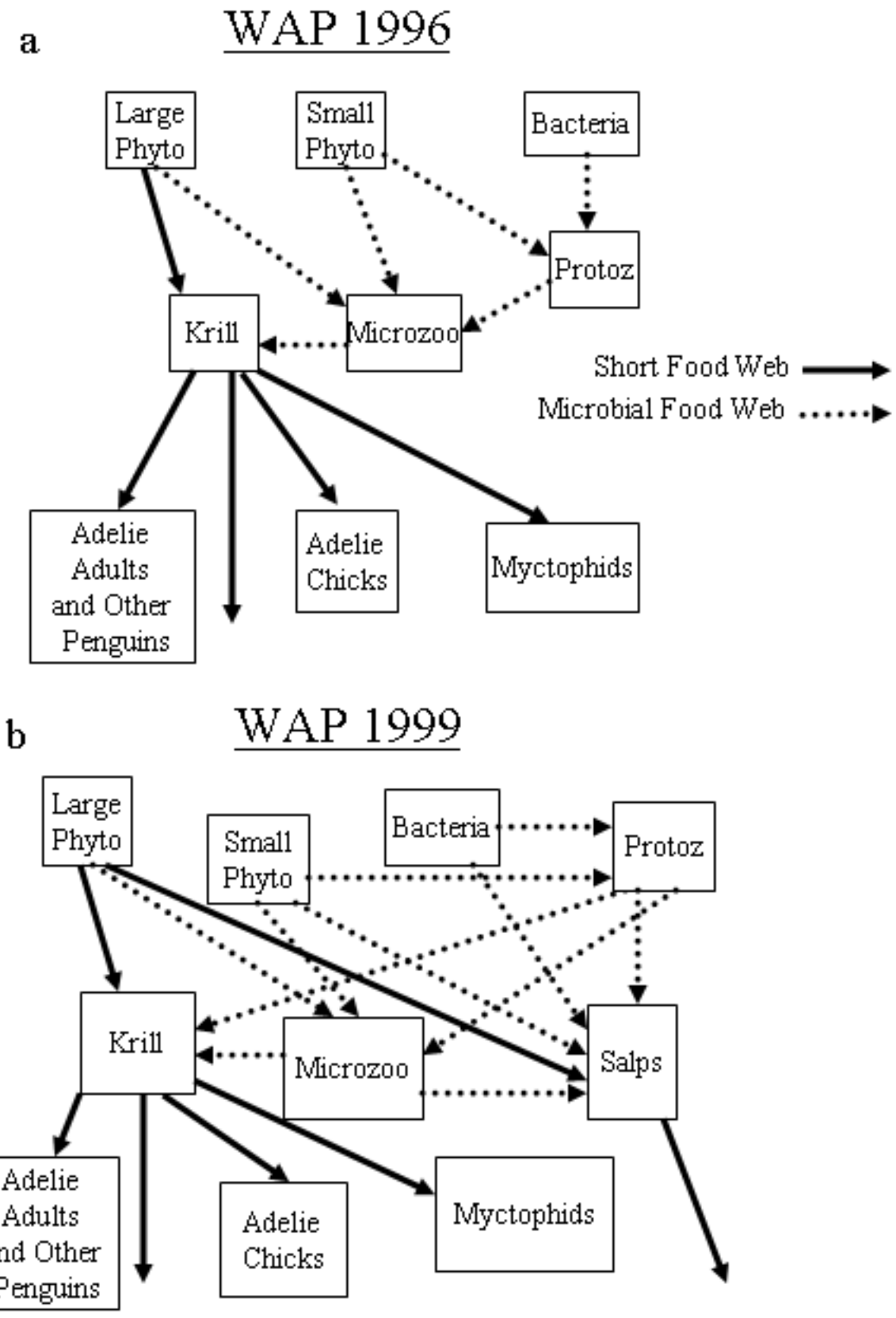
a
WAP 1996
Large Phyto
Small Phyto
Bacteria
Protoz
Krill
Microzoo
Short Food Web
Microbial Food Web
Adelie Adults and Other Penguins
Adelie Chicks
Myctophids
b
WAP 1999
Large Phyto
Small Phyto
Bacteria
Protoz
Krill
Microzoo
Salps
Adelie Adults and Other Penguins
Adelie Chicks
Myctophids

Figure 3

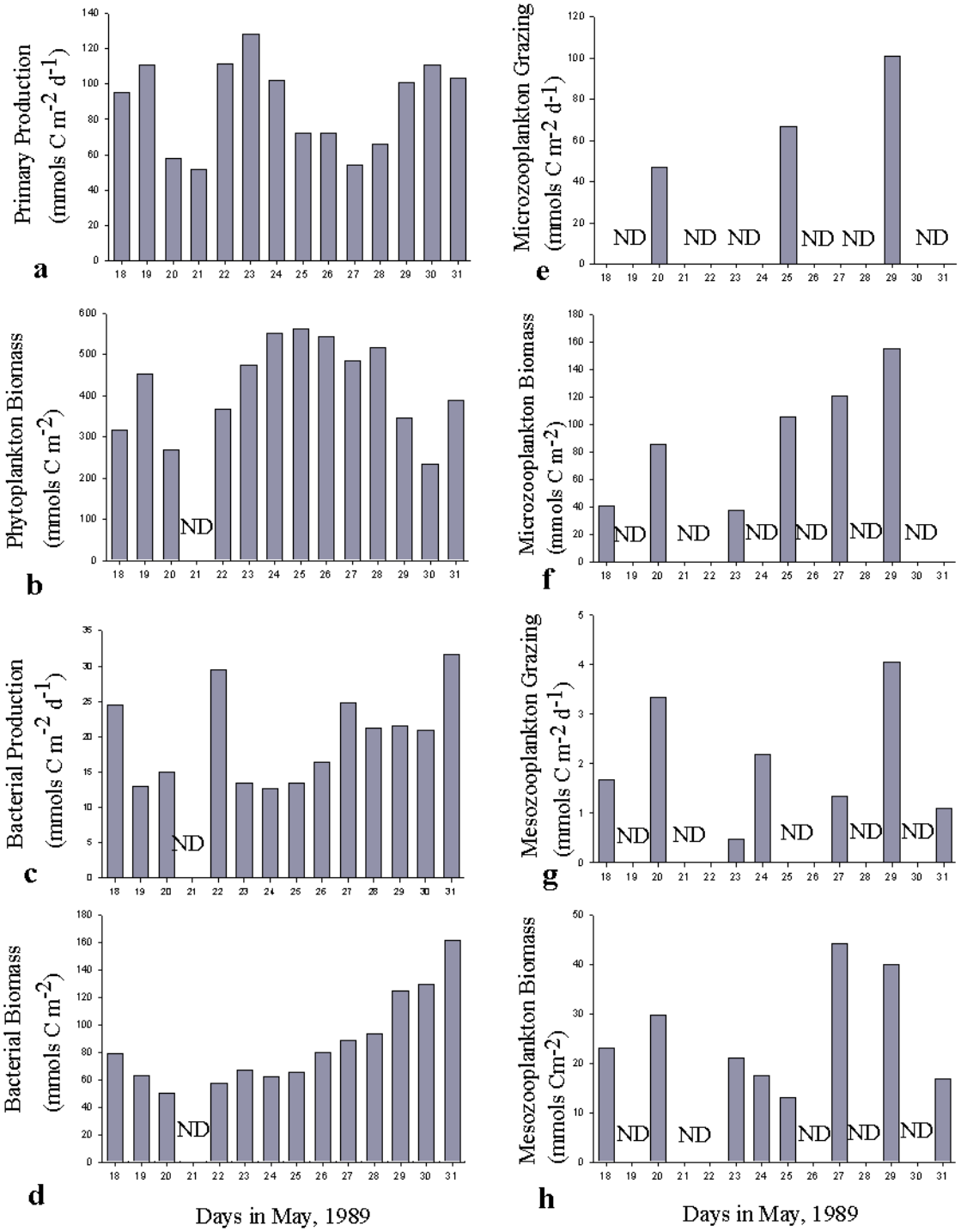
Primary Production (mmols C m-2 d-1)
a
Phytoplankton Biomass (mmols C m-2)
b
Bacterial Production (mmols C m-2 d-1)
c
Bacterial Biomass (mmols C m-2)
d
Days in May, 1989
Microzooplankton Grazing (mmols C m-2 d-1)
e
Microzooplankton Biomass (mmols C m-2)
f
Mesozooplankton Grazing (mmols C m-2 d-1)
g
Mesozooplankton Biomass (mmols Cm-2)
h
Days in May, 1989
ND

Figure 4

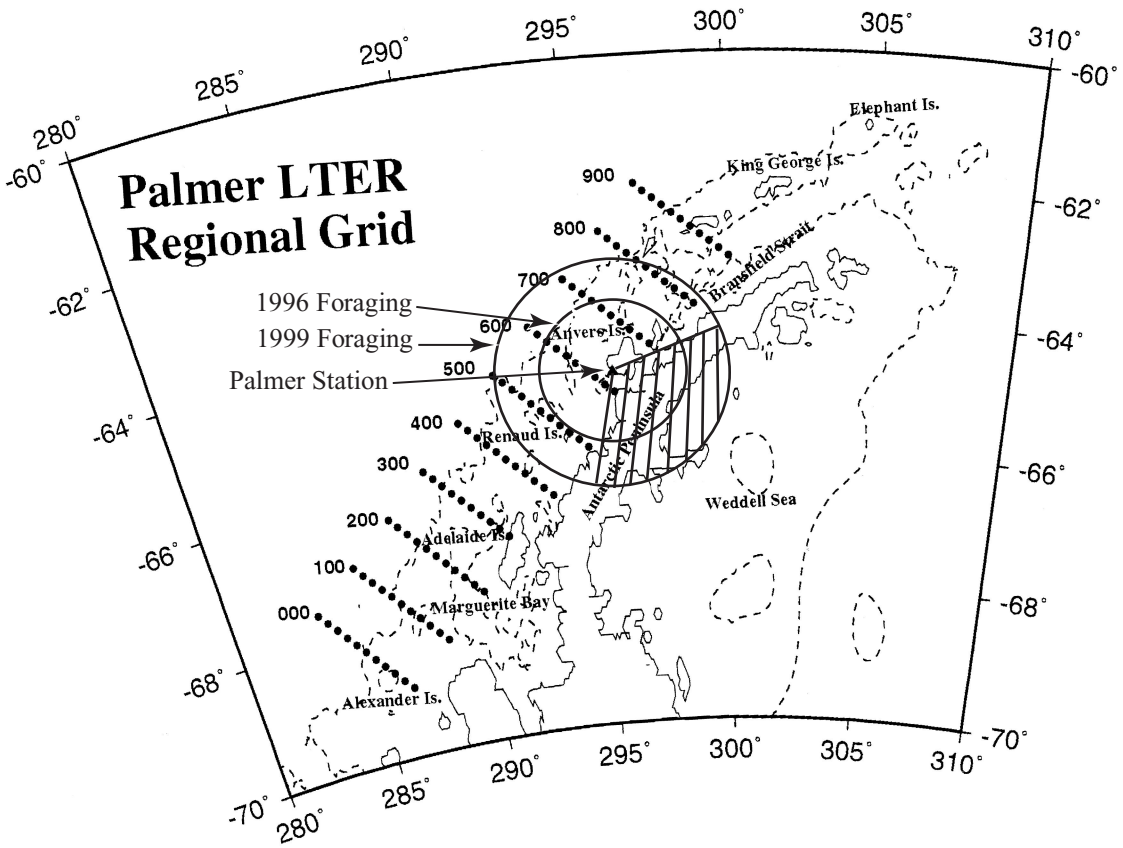
Palmer LTER
Regional Grid
1996 Foraging
1999 Foraging
Palmer Station
Elephant Is.
King George Is.
Bransfield Strait
Anvers Is.
Renaud Is.
Antarctic Peninsula
Weddell Sea
Adelaide Is.
Marguerite Bay
Alexander Is.
900
800
700
600
500
400
300
200
100
000
280°
285°
290°
295°
300°
305°
310°
-60°
-62°
-64°
-66°
-68°
-70°

Figure 5

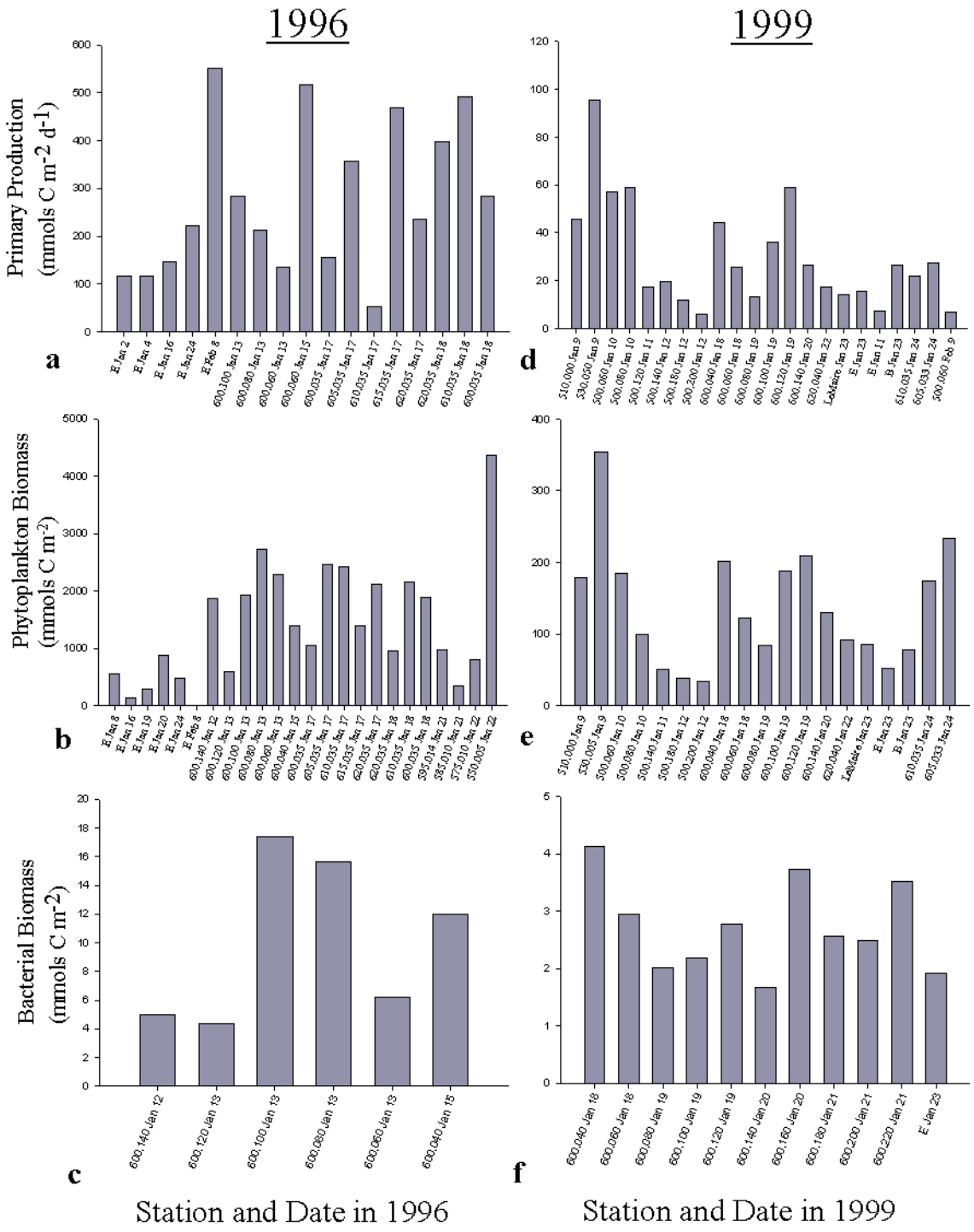
1996
1999
Primary Production (mmols C m-2 d-1)
Phytoplankton Biomass (mmols C m-2)
Bacterial Biomass (mmols C m-2)
a
b
c
d
e
f
Station and Date in 1996
Station and Date in 1999

Figure 6

a

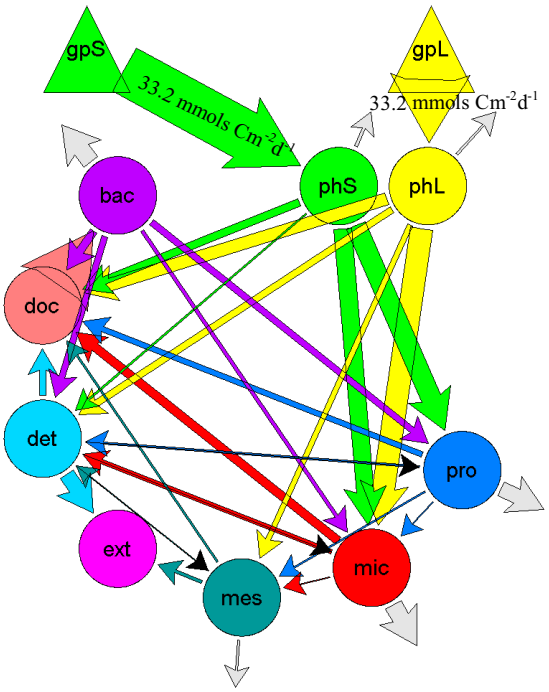

b

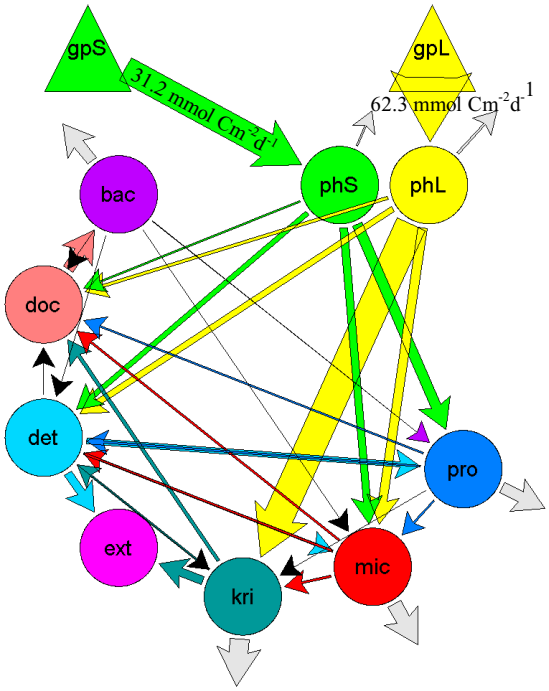

gpS = Gross PP for Small Phytoplankton

gpL = Gross PP for Large Phytoplankton

bac = Bacteria

det = Detritus

ext = External

mes = Mesozooplankton

kri = Krill

mic = Microzooplankton

pro = Protozoans

Figure 7

a

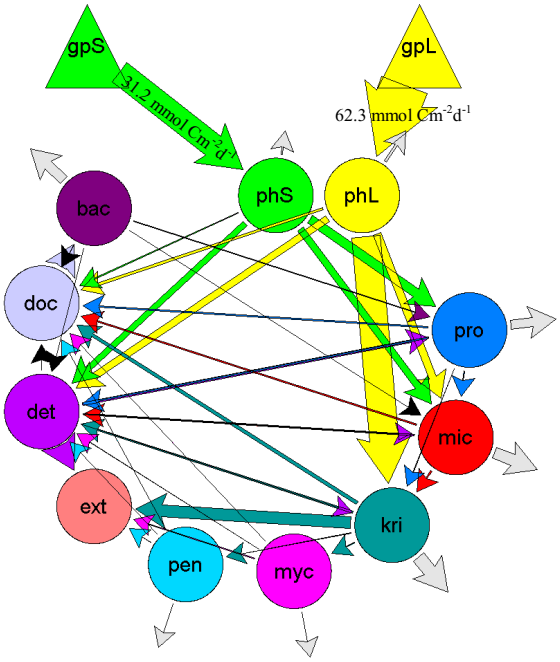

b

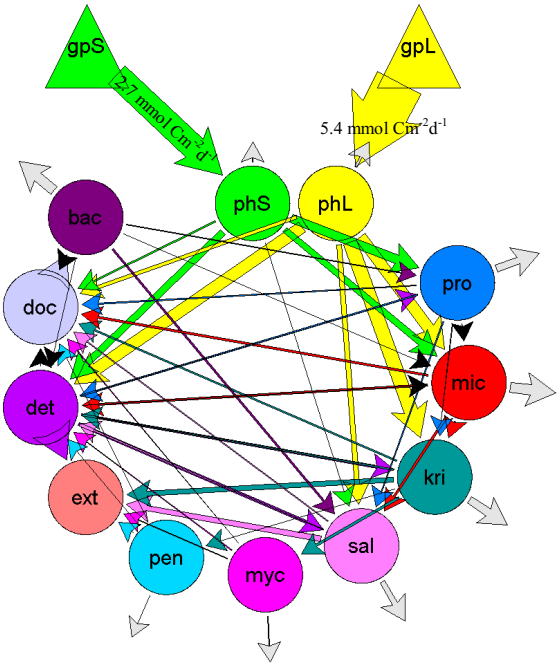

gpS = Gross PP for Small Phytoplankton

gpL = Gross PP for Large Phytoplankton

bac = Bacteria

det = Detritus

ext = External

mes = Mesozooplankton

kri = Krill

mic = Microzooplankton

pro = Protozoans

pen = Penguins

myc = Myctophids

Figure 8

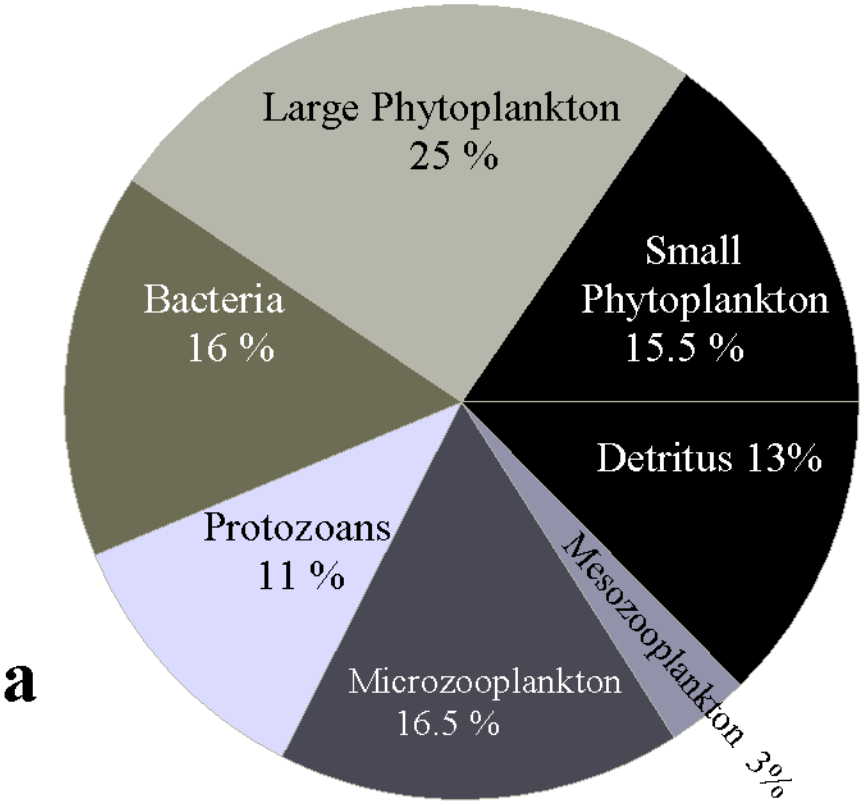
Large Phytoplankton
25 %
Small
Phytoplankton
15.5 %
Bacteria
16 %
Detritus 13%
Protozoans
11 %
Mesozooplankton 3%
Microzooplankton
16.5 %

a

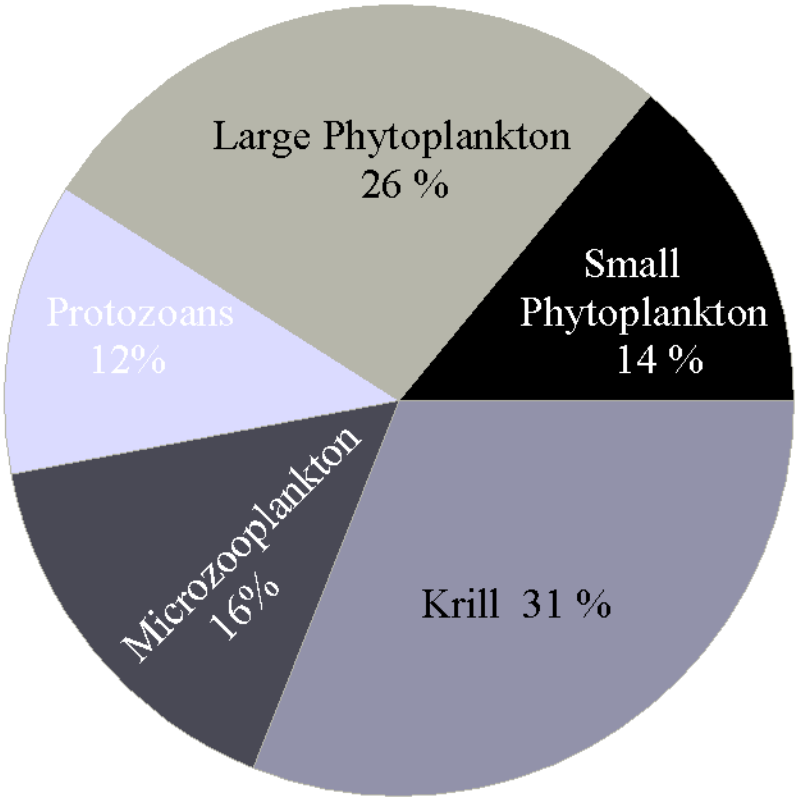
Large Phytoplankton
26 %
Small
Phytoplankton
14 %
Protozoans
12%
Microzooplankton
16%
Krill 31 %

b